

Generating cosmological perturbations in non-singular Horndeski cosmologies

Y. Ageeva^{a,b,c,1}, P. Petrov^{a,2}, V. Rubakov^{a,b,3}

^a *Institute for Nuclear Research of the Russian Academy of Sciences,
60th October Anniversary Prospect, 7a, 117312 Moscow, Russia*

^b *Department of Particle Physics and Cosmology,
Physics Faculty, M.V. Lomonosov Moscow State University,
Leninskie Gory 1-2, 119991 Moscow, Russia*

^c *Institute for Theoretical and Mathematical Physics,
M.V. Lomonosov Moscow State University,
Leninskie Gory 1, 119991 Moscow, Russia*

Abstract

We construct a concrete model of Horndeski bounce with strong gravity in the past. Within this model we show that the correct spectra of cosmological perturbations may be generated at early contracting epoch, with mild fine-tuning ensuring that the scalar spectral tilt n_S and tensor-to-scalar ratio r are consistent with observations. The smallness of r is governed by the smallness of the scalar sound speed. Arbitrarily small values of r are forbidden in our setup because of the strong coupling in the past. Nevertheless, we show that it is possible to generate perturbations in a controllable way, i.e. in the regime where the background evolution and perturbations are legitimately described within classical field theory and weakly coupled quantum theory.

1 Introduction

Nowadays a vigorous research of non-singular scenarios which are alternative or complementary to inflation continues. The realization of non-singular behaviour within classical field theory requires the violation of the null convergence condition (null energy condition (NEC))

¹**email:** ageeva@inr.ac.ru

²**email:** petrov@inr.ac.ru

³**email:** rubakov@inr.ac.ru

in General Relativity), see Ref. [1] for a review. However, models with unusual matter which violates the NEC or null convergence condition [2] often suffer from pathological behavior because of various kinds of instabilities. In Refs. [3–5] it was first shown, that stable violation of NEC can be implemented in Horndeski theories [6] (for reviews see, e.g., Refs. [1, 7]). Horndeski theory is a scalar-tensor modification of gravity. The Lagrangian of the latter contains second derivatives of both the metric and scalar field, but yet provides the second-order equations of motion. The explicit examples of healthy NEC-violating non-singular early stages, such as bouncing solutions [7–23] or Galilean genesis [3, 24–29] are numerous in Horndeski theory and its subclasses. In this paper we focus on bouncing Universe.

Yet another problem arises on the way to constructing the whole cosmological evolution of the Universe. Cosmologies which involve early non-singular epoch typically suffer from either singularities or gradient and/or ghost instabilities at some moment of time in the past or in the future (possibly well before or well after the bounce). Thus, even within Horndeski theories, extending bouncing cosmology to the whole time interval $-\infty < t < +\infty$ is not straightforward. Namely, perturbations about bouncing spatially flat FLRW backgrounds $ds^2 = -dt^2 + a^2(t)\delta_{ij}dx^i dx^j$ have either gradient or ghost instabilities, or both, provided that the following two integrals diverge:

$$\int_{-\infty}^t a(t)(\mathcal{F}_T + \mathcal{F}_S)dt = \infty , \quad (1a)$$

$$\int_t^{+\infty} a(t)(\mathcal{F}_T + \mathcal{F}_S)dt = \infty , \quad (1b)$$

where \mathcal{F}_T and \mathcal{F}_S are time-dependent coefficients in the quadratic actions for tensor (transverse traceless h_{ij}) and scalar (ζ) perturbations,

$$\mathcal{S}_{hh} = \int dt d^3x \frac{a^3}{8} \left[\mathcal{G}_T \dot{h}_{ij}^2 - \frac{\mathcal{F}_T}{a^2} h_{ij,k} h_{ij,k} \right] , \quad (2a)$$

$$\mathcal{S}_{\zeta\zeta} = \int dt d^3x a^3 \left[\mathcal{G}_S \dot{\zeta}^2 - \frac{\mathcal{F}_S}{a^2} \zeta_{,i} \zeta_{,i} \right] . \quad (2b)$$

This property, known as the no-go theorem [30–33], rules out the simplest bouncing Horndeski setups where $a(t)$ tends to infinity while \mathcal{F}_T and \mathcal{F}_S stay positive and finite as $t \rightarrow \pm\infty$.

One way [34–39] of getting around this theorem is to employ beyond Horndeski theories [40, 41] Degenerate Higher-Order Scalar-Tensor (DHOST) generalizations [42]. These, however, have their own problems, since adding conventional matter fields often results in superluminality [43]. Without employing these generalizations, i.e., staying within the Horndeski class, there is still a possibility to allow the coefficients \mathcal{G}_T , \mathcal{F}_T , \mathcal{G}_S and \mathcal{F}_S to tend to zero as $t \rightarrow -\infty$ in such a way that the integral in the left hand side of (1a) converges in the lower limit [31]. At first sight this is dangerous from the viewpoint of strong coupling: the

coefficients $\mathcal{G}_T, \mathcal{F}_T, \mathcal{G}_S$ and \mathcal{F}_S are analogs of the Planck mass squared, so their early-time behavior $\mathcal{G}_T, \mathcal{F}_T, \mathcal{G}_S, \mathcal{F}_S \rightarrow 0$ as $t \rightarrow -\infty$ implies that the gravitational interaction is strong in remote past; note that we always work in the Jordan frame and that $a(t)$ grows backwards in time at early times. Nevertheless, depending on the model, the cosmological evolution may, in fact, be legitimately described within classical field theory at all times, since even at early times the classical energy scale (which is $|t|^{-1}$ for power-law bounce) may be lower than the quantum strong coupling scale [44–47]. It is worth emphasizing that this idea of healthy bounce with “strong gravity in the past” (meaning that $\mathcal{G}_T, \mathcal{F}_T, \mathcal{G}_S, \mathcal{F}_S \rightarrow 0$ as $t \rightarrow -\infty$) has been re-invented, albeit not quite explicitly, in Refs. [48, 49] from a different perspective: bounce in the Jordan frame is obtained there via conformal transformation from an inflationary setup in the Einstein frame. Unlike in Refs. [48, 49], we work directly in the Jordan frame.

It is relatively straightforward to construct Horndeski models which admit bouncing solutions with power-law asymptotics at early times [31, 47],

$$a(t) \propto (-t)^\chi, \quad \mathcal{G}_T, \mathcal{F}_T, \mathcal{G}_S, \mathcal{F}_S \propto \frac{1}{(-t)^{2\mu}}, \quad t \rightarrow -\infty, \quad (3)$$

with time-independent parameters $1 > \chi > 0$, $2\mu > \chi + 1$. The latter property guarantees that the inequality (1a) does not hold, which is a pre-requisite for healthy bounce. In this paper we concentrate on this simple case and consider the generation of cosmological perturbations at early contraction stage. In terms of conformal time $\eta \propto -(-t)^{1-\chi}$, the quadratic action (2a) for tensor perturbations coincides with that in General Relativity with the background scale factor

$$a_E(\eta) = a(\eta)\mathcal{G}_T^{1/2}(\eta) \propto \frac{1}{(-\eta)^{\frac{\mu-\chi}{1-\chi}}}. \quad (4)$$

In fact, this is precisely the scale factor in the Einstein frame in our class of models. Now, for $\mu < 1$ the Einstein frame cosmic time $t_E = \int a_E(\eta)d\eta = -(-\eta)^{\frac{1-\mu}{1-\chi}}$ runs from $t_E = -\infty$, and the effective scale factor increases as $a_E = (-t_E)^{-b}$ where $b = \frac{\mu-\chi}{1-\mu} > 1$ [45]. Such a geometry is singular as $t_E \rightarrow -\infty$: it is past geodesically incomplete and cannot be completed¹. On the other hand, for $\mu > 1$ one immediately recognizes effective power-law inflation with

$$a_E(t_E) \propto t_E^{\frac{\mu-\chi}{\mu-1}}, \quad (5)$$

where $t_E \propto (-\eta)^{-\frac{\mu-1}{1-\chi}}$ runs from $t_E = 0$. In the Einstein frame, this is a version of G -inflation [5]. In either case, for $\mu \approx 1$ the Einstein frame expansion is nearly exponential, so the power spectrum of generated tensor perturbations is nearly flat; similar observation

¹This property is not pathological in our case, since by assumption particles with time-independent mass feel the Jordan frame geometry rather than the Einstein frame one.

applies to scalar perturbations as well. This implies that Horndeski bounce with “strong gravity in the past” may be capable of generating realistic cosmological perturbations; we again emphasize the similarity with Refs. [5,48,49] (where approximate flatness of the spectra is built in by construction).

In this paper we consider the models from the class of Refs. [31,47], as described below. The issues we would like to understand are: (i) what governs spectral tilts and the overall amplitudes of scalar and tensor perturbations; (ii) is it possible to obtain small tensor-to-scalar ratio $r = \mathcal{P}_h/\mathcal{P}_\zeta$ and, if so, what sort of tuning is required for that; (iii) is it possible to generate perturbations in a controllable way, i.e., in the regime where the background evolution and perturbations are legitimately described within classical field theory and weakly coupled quantum theory, respectively — and if so, does this constrain the values of observables.

We emphasize that we design and study our models in the Jordan frame where they have fairly simple structure. We could equivalently work in the Einstein frame, but then the analysis would be more cumbersome. We comment on the Einstein frame counterparts of our findings where appropriate.

An alert reader would anticipate that the spectral tilts (both scalar and tensor) are to large extent determined by the value of μ in (3); in particular, red tilts occur at $\mu > 1$. This is indeed the case, see Sec. 2.3. In this paper we mostly stick to the Λ CDM value of the scalar spectral index [50],

$$n_S = 0.9649 \pm 0.0042 . \tag{6}$$

We comment, however, that the possible presence of early dark energy makes the scale invariant Harrison–Zeldovich spectrum with $n_S = 1$ consistent with observations [51,52]. Hence, we also briefly consider a bounce model with the flat power spectrum.

This paper is organized as follows. We introduce our class of Horndeski models and discuss early contracting stage of bouncing universe in Secs. 2.1, 2.2. We derive the properties of linearized scalar and tensor perturbations generated at that stage in Sec. 2.3, while in Sec. 2.4 we point out the relation between the flatness of the spectra and approximate dilatation invariance of the models. Sections 2.5 and 2.6 are central in our relatively general discussion in Sec. 2: we observe that there is tension between the small value of r (and to lesser extent the red scalar spectral tilt), on the one hand, and the requirement of the absence of strong coupling, on the other. We consider this issue at qualitative level in Sec. 2.5 and proceed to quantitative analysis in Sec. 2.6. We illustrate this tension in Sec. 3, where we derive lower bounds on r in very concrete models, first with the Λ CDM scalar tilt (6), and then with $n_S = 1$. We conclude in Sec. 4. Appendices A, B, C contain details of more technical character. Appendix D is dedicated to the calculation of a specific form of covariant Lagrangian functions for our model. In Appendix E we proceed with conformal transformation of the metric and show how scale factor and Hubble parameter change after this transformation. Finally, Appendix F contains a concrete example of stable

and subluminal evolution, which starts from contraction, then bounce occurs and after that Universe turns into general relativity (GR) kination.

2 Horndeski models with power-law contraction

2.1 Preliminaries

We consider a subclass of Horndeski theories whose action has the form (in the Jordan frame)

$$\mathcal{S} = \int d^4x \sqrt{-g} \{ G_2(\phi, X) - G_3(\phi, X) \square \phi + G_4(\phi, X) R + G_{4X} [(\square \phi)^2 - (\nabla_\mu \nabla_\nu \phi)^2] \} , \quad (7)$$

$$X = -\frac{1}{2} g^{\mu\nu} \partial_\mu \phi \partial_\nu \phi ,$$

where $\square \phi = g^{\mu\nu} \nabla_\mu \nabla_\nu \phi$ and $(\nabla_\mu \nabla_\nu \phi)^2 = \nabla_\mu \nabla_\nu \phi \nabla^\mu \nabla^\nu \phi$, R is the Ricci scalar. The metric signature is $(-, +, +, +)$. Unlike the general Horndeski theory, the Lagrangian (7) involves three arbitrary functions $G_{2,3,4}$ rather than four. It is convenient to work in the ADM formalism [7]. To this end, the metric is written as

$$ds^2 = -N^2 d\hat{t}^2 + \gamma_{ij} (dx^i + N^i d\hat{t}) (dx^j + N^j d\hat{t}) ,$$

where γ_{ij} is three-dimensional metric, N is the lapse function and $N_i = \gamma_{ij} N^j$ is the shift vector. We denote the general time variable by \hat{t} and reserve the notation t for cosmic time. By choosing the unitary gauge (in which ϕ depends on \hat{t} only and has prescribed form $\phi = \phi(\hat{t})$), one rewrites the action as follows,

$$\mathcal{S} = \int d^4x \sqrt{-g} [A_2(\hat{t}, N) + A_3(\hat{t}, N) K + A_4(\hat{t}, N) (K^2 - K_{ij}^2) + B_4(\hat{t}, N) R^{(3)}] , \quad (8)$$

where

$$A_4(\hat{t}, N) = -B_4(\hat{t}, N) - N \frac{\partial B_4(\hat{t}, N)}{\partial N} ,$$

${}^{(3)}R_{ij}$ is the Ricci tensor made of γ_{ij} , $\sqrt{-g} = N \sqrt{\gamma}$, $K = \gamma^{ij} K_{ij}$, ${}^{(3)}R = \gamma^{ij} {}^{(3)}R_{ij}$ and

$$K_{ij} \equiv \frac{1}{2N} \left(\frac{d\gamma_{ij}}{d\hat{t}} - {}^{(3)}\nabla_i N_j - {}^{(3)}\nabla_j N_i \right) ,$$

is extrinsic curvature of hypersurfaces $\hat{t} = \text{const.}$ The relationship between the Lagrangian functions in the covariant and ADM formalisms is given by [41, 53, 54]

$$G_2 = A_2 - 2XF_\phi, \quad G_3 = -2XF_X - F, \quad G_4 = B_4 , \quad (9)$$

where N and X are related by

$$N^{-1} d\phi / d\hat{t} = \sqrt{2X} , \quad (10)$$

and

$$F_X = -\frac{A_3}{(2X)^{3/2}} - \frac{B_{4\phi}}{X}. \quad (11)$$

We note in passing a subtlety here. Equation (11) defines $F(\phi, X)$ up to additive term $D(\phi)$. This term modifies the Lagrangian functions,

$$G_2 \rightarrow G_2 - 2XD_\phi, \quad G_3 \rightarrow G_3 - D.$$

However, the additional contribution to the action (7) vanishes upon integration by parts,

$$\int d^4x \sqrt{-g} (-2XD_\phi + D\Box\phi) = \int d^4x \sqrt{-g} \nabla_\mu (D\nabla^\mu\phi) = 0. \quad (12)$$

Therefore, this freedom is, in fact, irrelevant.

To describe FLRW background and perturbations about it, one writes

$$N = N_0(\hat{t})(1 + \alpha), \quad (13a)$$

$$N_i = \partial_i\beta + N_i^T, \quad (13b)$$

$$\gamma_{ij} = a^2(\hat{t}) \left(e^{2\zeta} (e^h)_{ij} + \partial_i\partial_j Y + \partial_i W_j^T + \partial_j W_i^T \right), \quad (13c)$$

where $a(\hat{t})$ and $N_0(\hat{t})$ are background solutions, $\partial_i N^{Ti} = 0$ and

$$(e^h)_{ij} = \delta_{ij} + h_{ij} + \frac{1}{2}h_{ik}h_{kj} + \frac{1}{6}h_{ik}h_{kl}h_{lj} + \dots, \quad h_{ii} = 0, \quad \partial_i h_{ij} = 0.$$

Throughout this paper, we denote the background lapse function by N instead of N_0 . The residual gauge freedom is fixed by setting $Y = 0$ and $W_i^T = 0$. Variables α , β and N_i^T enter the action without temporal derivatives; the dynamical degrees of freedom are ζ and transverse traceless h_{ij} , i.e., scalar and tensor perturbations. Upon integrating out variables α and β , one obtains the quadratic actions for scalar and tensor perturbations [29]

$$\mathcal{S}_{\zeta\zeta}^{(2)} = \int d\hat{t} d^3x N a^3 \left[\frac{\mathcal{G}_S}{N^2} \left(\frac{\partial\zeta}{\partial\hat{t}} \right)^2 - \frac{\mathcal{F}_S}{a^2} \left(\vec{\nabla}\zeta \right)^2 \right], \quad (14a)$$

$$\mathcal{S}_{hh}^{(2)} = \int d\hat{t} d^3x \frac{N a^3}{8} \left[\frac{\mathcal{G}_T}{N^2} \left(\frac{\partial h_{ij}}{\partial\hat{t}} \right)^2 - \frac{\mathcal{F}_T}{a^2} h_{ij,k} h_{ij,k} \right]. \quad (14b)$$

Explicit expressions for the coefficients \mathcal{G}_S , \mathcal{F}_S , \mathcal{G}_T , and \mathcal{F}_T in general models of the type (8) as well as equations for background are collected in Appendix A.

2.2 Power-law contraction

To build a bouncing model with the early-time behavior (3), we choose the following form [47] of the Lagrangian functions in (8) at early times, $t \rightarrow -\infty$:

$$A_2(\hat{t}, N) = \hat{g}(-\hat{t})^{-2\mu-2} \cdot a_2(N) , \quad (15a)$$

$$A_3(\hat{t}, N) = \hat{g}(-\hat{t})^{-2\mu-1} \cdot a_3(N) , \quad (15b)$$

$$A_4 = A_4(\hat{t}) = -B_4(\hat{t}) = -\frac{\hat{g}}{2}(-\hat{t})^{-2\mu} , \quad (15c)$$

where \hat{g} is some positive constant. Then the equations for background, eqs. (71), take the following form

$$\begin{aligned} \frac{(Na_2)_N}{(-\hat{t})^2} + \frac{3Na_3NH}{(-\hat{t})} + 3H^2 &= 0 , \\ \frac{a_2}{(-\hat{t})^2} + 3H^2 - \frac{1}{N} \left[\frac{(2\mu+1)a_3}{(-\hat{t})^2} - \frac{4\mu H}{(-\hat{t})} - 2\frac{dH}{d\hat{t}} + \frac{a_{3N}}{(-\hat{t})} \frac{dN}{d\hat{t}} \right] &= 0 , \end{aligned}$$

where H is the physical Hubble parameter. We make use of the *Ansatz*

$$N = \text{const} , \quad a = d(-t)^\chi , \quad (17)$$

where $\chi > 0$ is a constant and $t = N\hat{t}$ is cosmic time, so that $H = \chi/t$, and find the algebraic equations for N and χ :

$$(Na_2)_N - 3\chi a_{3N} + 3\frac{\chi^2}{N^2} = 0 , \quad (18a)$$

$$a_2 - \frac{1}{N}(2\mu+1)\left(a_3 + 2\frac{\chi}{N}\right) + 3\frac{\chi^2}{N^2} = 0 . \quad (18b)$$

In what follows we assume that these equations have a solution with $N > 0$ and $1 > \chi > 0$ (the reason for requiring that $\chi < 1$ will become clear shortly, see also eq. (4)).

Let us emphasize that the form of the Lagrangian functions (15), as well as the entire discussion in this paper, refer to the early contraction stage only. To obtain the bounce itself, as well as subsequent expansion stage, one has to make use of more sophisticated Lagrangian functions that can be obtained, e.g., by gluing procedure elaborated in Ref. [47]. A lesson from Ref. [47] is that designing stable bouncing models with given early-time asymptotics with “strong gravity in the past” is relatively straightforward. In this paper we do not aim at constructing complete cosmological models and stick to early times when the cosmological perturbations are supposed to be generated.

The coefficients entering the quadratic actions (14) for perturbations are straightforwardly calculated by making use of the general expressions (72), (73). In what follows it

is convenient to work in cosmic time $t = N\hat{t}$ and write the quadratic actions in convenient forms (hereafter dot denotes the derivative with respect to cosmic time t)

$$\mathcal{S}_{hh} = \int dt d^3x \frac{a^3}{8} \left[\mathcal{G}_T \dot{h}_{ij}^2 - \frac{\mathcal{F}_T}{a^2} h_{ij,k} h_{ij,k} \right], \quad (19a)$$

$$\mathcal{S}_{\zeta\zeta} = \int dt d^3x a^3 \left[\mathcal{G}_S \dot{\zeta}^2 - \frac{\mathcal{F}_S}{a^2} \zeta_{,i} \zeta_{,i} \right]. \quad (19b)$$

Then

$$\mathcal{G}_T = \mathcal{F}_T = \frac{g}{(-t)^{2\mu}}, \quad (20)$$

where

$$g = N^{2\mu} \hat{g}, \quad (21)$$

and

$$\mathcal{G}_S = g \frac{g_S}{2(-t)^{2\mu}}, \quad \mathcal{F}_S = g \frac{f_S}{2(-t)^{2\mu}}, \quad (22)$$

with

$$f_S = \frac{2(2 - 4\mu + N^2 a_{3N})}{2\chi - N^2 a_{3N}}, \quad (23a)$$

$$g_S = 2 \left[\frac{2 \left(2N^3 a_{2N} + N^4 a_{2NN} - 3\chi(2\chi + N^3 a_{3NN}) \right)}{(N^2 a_{3N} - 2\chi)^2} + 3 \right], \quad (23b)$$

where $a_{2,3}(N)$ and their derivatives are to be evaluated on the solution to eqs. (18), so that g , f_S and g_S are independent of time. Note that the propagation of the tensor perturbations is luminal,

$$u_T^2 = \frac{\mathcal{F}_T}{\mathcal{G}_T} = 1,$$

whereas the sound speed in the scalar sector is given by

$$u_S^2 = \frac{\mathcal{F}_S}{\mathcal{G}_S} = \frac{f_S}{g_S}, \quad (24)$$

and can be substantially smaller than 1.

To end up this Section, we notice that the conformal transformation

$$g_{\mu\nu} = \frac{M_P^2}{2B_4} g_{\mu\nu}^{(E)}, \quad (25)$$

where $M_P = (8\pi G)^{-1/2}$ is the reduced Planck mass, converts the theory into the Einstein frame. In the Einstein frame, the action is cubic Horndeski, and the scale factor is given by eq. (4). This justifies the discussion in Sec. 1 after eq. (4).

2.3 Generating perturbations

As pointed out in Introduction, the quadratic actions for perturbations coincide (modulo the fact that $u_S^2 \neq 1$) with the action for tensor perturbation in power-law expansion setup. So, the cosmological perturbations with nearly flat power spectrum may be generated at early contraction epoch. Let us consider for definiteness scalar perturbation ζ . It obeys the linearized equation

$$\ddot{\zeta} + \frac{2\mu - 3\chi}{|t|} \dot{\zeta} + \frac{u_S^2 k^2}{d^2 |t|^{2\chi}} \zeta = 0, \quad (26)$$

For $0 < \chi < 1$, the mode is effectively subhorizon at early times (in the sense that the effective Hubble time scale $|t|$ is greater than the period of oscillations $d \cdot |t|^\chi / (u_S k)$), so it is adequately described within the WKB approximation. At later times, the mode is superhorizon; in what follows we consider the case

$$2\mu - 3\chi > 0, \quad (27)$$

in which the superhorizon mode experiences the Hubble friction and freezes out. The horizon exit occurs at time $t_f(k)$ when

$$\frac{2\mu - 3\chi}{|t_f|} \sim \frac{u_S k}{d |t_f|^\chi},$$

i.e.,

$$|t_f|(k) \sim \left[\frac{d}{k} \cdot \frac{(2\mu - 3\chi)}{u_S} \right]^{\frac{1}{1-\chi}}. \quad (28)$$

Thus, once the parameters of the theory are chosen in such a way that $1 > \chi > 0$, $2\mu - 3\chi > 0$, the perturbations are generated in a straightforward way, *provided that the weak coupling regime occurs all the way down to $|t| \sim |t_f|$.*

Let us also discuss a constraint that has to do with the Belinsky–Khalatnikov–Lifshitz phenomenon [55–57]. In our model this phenomenon manifests itself in the behavior of superhorizon tensor (and also scalar) modes in the contracting Universe: in the BKL case, one of the two solutions for a superhorizon mode of given conformal momentum grows as t increases and diverges in the formal limit $t \rightarrow 0$, while another solution stays constant in time. This means that the Universe becomes strongly anisotropic and inhomogeneous at late times, which is undesirable (see, e.g., Ref. [58] for discussion). In order to avoid BKL, one makes sure that the time-dependent superhorizon solution decays, instead of growing, as t increases towards zero. In our framework, the equation of motion for superhorizon perturbation is obtained from (19a) with spatial derivatives neglected,

$$\frac{1}{a^3 \mathcal{G}_T} \frac{d}{dt} \left(a^3 \mathcal{G}_T \dot{h}_{ij} \right) = 0.$$

One of its solutions is constant in time, while another is

$$h_{ij} \propto \int dt \frac{1}{a^3 \mathcal{G}_T} \propto (-t)^{2\mu-3\chi+1}.$$

It decays as t increases towards zero for

$$2\mu + 1 > 3\chi. \quad (29)$$

This constraint ensures also that the BKL phenomenon is absent for scalar perturbations. Recall that we choose the following constraints on parameters $\mu > 1$ and $\chi < 1$ in our model, thus the condition (29) is surely satisfied.

We outline the calculation in Appendix B, and here we give the results for the power spectra:

$$\mathcal{P}_\zeta \equiv \mathcal{A}_\zeta \left(\frac{k}{k_*} \right)^{n_S-1}, \quad \mathcal{P}_T \equiv \mathcal{A}_T \left(\frac{k}{k_*} \right)^{n_T}, \quad (30)$$

where k_* is pivot scale, the spectral tilts are

$$n_S - 1 = n_T = 2 \cdot \left(\frac{1 - \mu}{1 - \chi} \right), \quad (31)$$

and the amplitudes are given by

$$\mathcal{A}_\zeta = \frac{1}{g} \cdot \frac{1}{g_S u_S^{2\nu}} \frac{(1 - \chi)^{2\frac{\mu-\chi}{1-\chi}}}{\pi \sin^2(\nu\pi) \Gamma^2(1 - \nu)} \left(\frac{k_*}{2d} \right)^{2\frac{1-\mu}{1-\chi}}, \quad (32a)$$

$$\mathcal{A}_T = \frac{8}{g} \cdot \frac{(1 - \chi)^{2\frac{\mu-\chi}{1-\chi}}}{\pi \sin^2(\nu\pi) \Gamma^2(1 - \nu)} \left(\frac{k_*}{2d} \right)^{2\frac{1-\mu}{1-\chi}}, \quad (32b)$$

where

$$\nu = \frac{1 + 2\mu - 3\chi}{2(1 - \chi)} = \frac{3}{2} + \frac{1 - n_S}{2}. \quad (33)$$

We immediately see from eqs. (32) that the smallness of the scalar and tensor amplitudes is guaranteed by the large value of the overall pre-factor \hat{g} in eqs. (15), and hence the factor g given by (21). Also, we see from (32) that the tensor-to-scalar ratio in our model is

$$r = \frac{\mathcal{A}_T}{\mathcal{A}_\zeta} = 8 \frac{f_S^\nu}{g_S^{\nu-1}} = 8 g_S u_S^{2\nu}. \quad (34)$$

This shows that it is not straightforward to have a small value of r , as required by observations [50, 59, 60], which give

$$r < 0.032.$$

Since $f_S \leq g_S$ to avoid superluminality, small r requires that either $f_S \leq g_S \ll 1$ or $u_S \ll 1$ or both. It is clear from (23) that obtaining both $g_S \ll 1$ and $f_S \ll 1$ requires strong

fine-tuning. On the contrary, eq. (23a) suggests that ensuring that $f_S \ll 1$ while $g_S \sim 1$, and hence $u_S^2 \ll 1$ may not be so problematic. We give concrete examples in Sec. 3. Thus, the small tensor-to-scalar ratio in our set of models is due to small sound speed of scalar perturbations. This is reminiscent of the situation in k-inflation [61–63], where the tensor-to-scalar ratio is also suppressed for small u_S .

We now turn to the scalar and tensor tilts given by eq. (31). First, we note that the two tilts are equal to each other, unlike in most of inflationary models. Second, we point out that approximate flatness of the spectra is ensured in our set of models by choosing $\mu \approx 1$, while the slightly red Λ CDM spectrum (6) is found for

$$\mu > 1 .$$

As we discuss below, the small value of r , especially in the case $\mu > 1$, is non-trivial from the viewpoint of the strong coupling problem. Before coming to the strong coupling issue, let us make a point on approximate flatness itself.

2.4 Flatness of power spectra and dilatation invariance

Flatness of the power spectra at $\mu = 1$ is not an accident: the model with $\mu = 1$ is invariant under scale transformations. Let us see this explicitly.

One immediately observes that for $\mu = 1$, the ADM action (8) with the Lagrangian functions given by (15) is invariant under scale transformation

$$\hat{t} = \lambda \hat{t}' , \quad x^i = \lambda x'^i , \quad (N, N_i, \gamma_{ij})(x^i, \hat{t}) = (N', N'_i, \gamma'_{ij})(x'^i, \hat{t}') , \quad (35)$$

with $\lambda = \text{const}$. However, in the ADM language this is a somewhat murky point. To clarify it, we move to covariant formalism with the action (7). To this end, we define the field ϕ , without loss of generality, in such a way that

$$-\hat{t} = e^{-\phi} .$$

Then eq. (10) gives

$$N = \frac{e^\phi}{\sqrt{2X}} , \quad (36)$$

and the Lagrangian functions take the following forms

$$A_2 = \hat{g} e^{(2\mu+2)\phi} a_2 \left(\frac{e^\phi}{\sqrt{2X}} \right) , \quad (37a)$$

$$A_3 = \hat{g} e^{(2\mu+1)\phi} a_3 \left(\frac{e^\phi}{\sqrt{2X}} \right) , \quad (37b)$$

$$A_4 = -\frac{\hat{g}}{2} e^{2\mu\phi} . \quad (37c)$$

They define the Lagrangian functions G_2, G_3, G_4 in accordance with eqs. (9) and (11). We put full expressions for these functions G_2, G_3, G_4 and some helpful calculations in Appendix D.

Now, in covariant formalism we introduce the scale transformation of metric and scalar field,

$$g_{\mu\nu} = \lambda^2 g'_{\mu\nu}, \quad \phi = \phi' - \ln \lambda, \quad (38)$$

so that $X = \lambda^{-2} X'$. The combination in the right hand side of eq. (36) is invariant under this transformation. The meaning of this property is that $N' = \frac{e^{\phi'}}{\sqrt{2X'}}$ (which is actually equal to N) is the lapse function in coordinates x'^{μ} introduced in (35). With this understanding, it is fairly straightforward to check that the action (7) with $\mu = 1$ is invariant under scale transformation (38). This is clear from the fact that under scale transformation one has

$$A_2(\phi, X) = \lambda^{-2\mu-2} A_2(\phi', X'), \quad A_3(\phi, X) = \lambda^{-2\mu-1} A_3(\phi', X'), \quad B_4(\phi) = \lambda^{-2\mu} B_4(\phi'),$$

and $\square\phi = \lambda^{-2}\square'\phi'$, $R = \lambda^{-2}R'$. A subtlety here concerns the function F . Its derivative F_X transforms as $F_X = \lambda^{2-2\mu} F'_{X'}$, as it should, so that one would think that

$$F = \int F_X dX = \lambda^{-2\mu} \int F'_{X'} dX' = \lambda^{-2\mu} F'.$$

This is not quite true, though. F_X defined by eq. (11) may contain a term $ce^{2\mu\phi}X^{-1}$, i.e., F may contain a term $ce^{2\mu\phi}\ln X$. Then, upon scaling transformation, function F , and hence functions G_2 and G_3 obtain log- λ terms,

$$(G_2)_{log} = -4c\mu X' e^{2\mu\phi'} \cdot \lambda^{-2\mu-2} \ln \lambda^{-2}, \quad (G_3)_{log} = -c e^{2\mu\phi'} \cdot \lambda^{-2\mu} \ln \lambda^{-2}.$$

However, their contribution to the action (7) vanishes upon integration by parts, in the same way as in eq. (12). Modulo this subtlety, the functions G_2, G_3, G_4 defined by eqs. (9) and (11), have correct scaling at $\mu = 1$ which ensures the scale invariance of the theory in covariant formulation.

2.5 Tension between small r and strong coupling: preliminaries

In this Section, we discuss in general terms the problematic issue with our mechanism of the generation of the cosmological perturbations at Horndeski bounce. It has to do with the dangerous strong coupling, on the one hand, and the small value of r , on the other — especially for positive $(\mu - 1)$ as required for the red scalar tilt. Using a concrete example, we will see in Sec. 3 that the problem may be overcome, but in a quite narrow range of parameters. This makes our mechanism particularly interesting and falsifiable.

In this Section we mostly consider for definiteness the case $\mu > 1$, as required by the Λ CDM value of the scalar spectral index (6), see eq. (32a). Our formulas, however, are valid

also in the Harrison–Zeldovich case $\mu = 1$, $n_S = 1$. We make specific comments on the latter case in appropriate places.

Taken literally, the model with $\mu > 1$ suffers strong coupling problem in the asymptotic past, $t \rightarrow -\infty$. This has been discussed in detail in Ref. [47] (see also Refs. [44–46]); here we sketch the argument.

The characteristic classical energy scale in the power-law bounce model is the inverse time scale of evolution,

$$E_{class}(t) = |t|^{-1} .$$

Indeed, both background values of physical quantities and parameters governing the perturbations evolve in power-law manner and get order 1 changes in time interval of order $|t|$ (as an exception, this does not apply to the scale factor $a(t)$ for $\chi \ll 1$, but does apply to the Hubble parameter, since $|\dot{H}/H| \sim |t|^{-1}$). To see whether this classical energy scale is lower than the quantum strong coupling scale, one has to estimate the latter.

Let us consider first the tensor sector of the model. Its quadratic action is given by eq. (19a); importantly, the coefficient $\mathcal{G}_T = \mathcal{F}_T$ tends to zero as $t \rightarrow -\infty$, see (20). The cubic action reads [64]

$$\mathcal{S}_{hhh}^{(3)} = \int dt a^3 d^3x \left[\frac{\mathcal{F}_T}{4a^2} \left(h_{ik}h_{jl} - \frac{1}{2}h_{ij}h_{kl} \right) h_{ij,kl} \right] . \quad (39)$$

Thus, the quantum strong coupling energy scale E_{strong} in the tensor sector is determined by the behavior of \mathcal{F}_T . To estimate this scale at a given moment of time, we note first that we can rescale spatial coordinates at that moment of time to set

$$a = 1 .$$

Now, if the strong coupling scale E_{strong} is much higher than the energy scale $|t|^{-1}$ of the classical evolution, the background can be treated as slowly varying, and at a given moment of time it is natural to introduce canonically normalized field $h_{ij}^{(c)}$ by

$$h_{ij} = \mathcal{G}_T^{-1/2} h_{ij}^{(c)} .$$

Then the cubic interaction term becomes

$$\mathcal{S}_{hhh}^{(3)} = \int dt d^3x \left[\frac{\mathcal{F}_T}{4\mathcal{G}_T^{3/2}} \left(h_{ik}^{(c)}h_{jl}^{(c)} - \frac{1}{2}h_{ij}^{(c)}h_{kl}^{(c)} \right) \partial_k \partial_l h_{ij}^{(c)} \right] .$$

On dimensional grounds, the quantum strong coupling scale is estimated as

$$E_{strong}^{TTT} \sim \frac{\mathcal{G}_T^{3/2}}{\mathcal{F}_T} = \frac{g^{1/2}}{|t|^\mu} , \quad (40)$$

where we use (20). This scale is indeed higher than the classical energy scale $H \sim |t|^{-1}$ provided that

$$|t|^{2\mu-2} < g. \quad (41)$$

As pointed out in Refs. [44–47], this inequality is indeed valid at arbitrarily large $|t|$ for $\mu < 1$, but *it does not hold in the asymptotic past* for $\mu > 1$, as required for the red spectral tilt.

Thus, there is potential tension between the red tilt and the validity of the (semi-)classical field theory treatment, i.e., absence of strong coupling. One may take various attitudes towards this potential problem. First, one may pretend to be ignorant about the situation at very early times, and consider only the evolution at the epoch when the theory is weakly coupled, in the sense that $|t|^{-1} < E_{strong}$. Second, one may think of a slow change of the exponent $\mu = \mu(t)$ from $\mu < 1$ in the asymptotic past to $\mu > 1$ at later times, when the perturbations are generated. In any case, however, our calculation of the power spectra in Sec. 2.3 and Appendix B is valid *provided that the WKB evolution before the exit from effective horizon occurs in the weak coupling regime*. This means that the freeze-out time (28) must obey the weak coupling condition (41) for any relevant momentum k .

In fact, the tensor sector is not problematic in this regard. To see this, we recall that the tensor modes exit the effective horizon at

$$t_f^{(T)}(k) \sim \left(\frac{d}{k}\right)^{\frac{1}{1-x}},$$

(see eq. (28) with $u_S = 1$ for tensor modes). Then the relation (41) with $t = t_f^{(T)}$ becomes

$$\frac{1}{g} \left(\frac{d}{k}\right)^{2\frac{\mu-1}{1-x}} \ll 1.$$

The left hand side here is of the order of the tensor amplitude \mathcal{A}_T , eq. (32b), so that the absence of strong coupling at the horizon exit time is guaranteed by the smallness of the tensor amplitude.

The latter property is actually obvious from the Einstein frame viewpoint. For $\mu > 1$, the Einstein frame universe experiences the power-law inflation (5). Strong coupling in the asymptotics $t \rightarrow -\infty$ ($t_E \rightarrow 0$) is interpreted as a mere fact that the inflationary Hubble parameter $H_E \sim t_E^{-1}$ formally exceeds M_P at small t_E . Now, the tensor amplitude is of order H_E^2/M_P^2 at the exit time from the inflationary horizon; small tensor amplitude means the absence of strong coupling at that time, $H_E \ll M_P$.

In the case $\mu = 1$, the condition of validity of the classical description is time-independent,

$$g \gg 1.$$

Again, this condition is automatically satisfied provided that the tensor amplitude (32b) is small.

The situation is more subtle in the scalar sector, since the scalar sound speed u_S is small, as required by the small tensor-to-scalar ratio (see eq. (34)). To appreciate this new aspect, we consider scalar perturbations whose quadratic action is given by (19b), i.e.,

$$\mathcal{S}_{\zeta\zeta} = \int dt d^3x a^3 \mathcal{G}_S \left[\dot{\zeta}^2 - \frac{u_S^2}{a^2} \zeta_{,i} \zeta_{,i} \right].$$

Hereafter we assume, in view of the above discussion, that g_S in eqs. (22), (23b) is of order 1, and the smallness of u_S is due to small f_S . Cubic terms in the action for ζ are calculated in Refs. [65–68]. As we discuss in Sec. 2.6.3 and Appendix C, the most relevant terms reduce to just one term (76) in the cubic action (with $a = 1$, as before):

$$\mathcal{S}_{\zeta\zeta\zeta}^{(3)} = \int dt d^3x \Lambda_\zeta \partial^2 \zeta (\partial_i \zeta)^2, \quad (42)$$

with

$$\Lambda_\zeta = \frac{\mathcal{G}_T^3}{4\Theta^2},$$

where $\partial^2 = \partial_i \partial_i$, and Θ is given by (74b). In our model (15), we have

$$\Theta = g \frac{\vartheta}{|t|^{2\mu+1}}, \quad \vartheta = \frac{1}{2} N^2 a_{3N} - \chi, \quad (43)$$

Thus,

$$\Lambda_\zeta = g \frac{\lambda_\zeta}{|t|^{2\mu-2}},$$

where²

$$\lambda_\zeta = \frac{1}{4\vartheta^2} = O(1), \quad (44)$$

for all values of u_S including $u_S \ll 1$. To get rid of the sound speed in the quadratic part of the action, we not only set $a = 1$, but rescale the spatial coordinates further, $x^i = u_S y^i$. Upon introducing canonically normalized field

$$\zeta^{(c)} = (2\mathcal{G}_S)^{1/2} u_S^{3/2} \zeta,$$

we obtain the quadratic action in canonical form (with effective sound speed equal to 1), whereas the cubic action becomes

$$\mathcal{S}_{\zeta\zeta\zeta}^{(3)} = \int dt d^3y \Lambda_\zeta (2\mathcal{G}_S)^{-3/2} u_S^{-11/2} \partial_y^2 \zeta^{(c)} (\partial_y \zeta^{(c)})^2. \quad (45)$$

²In the model of Sec. 3 the property $\lambda_\zeta = O(1)$ is valid provided that χ is not fine tuned to be very close to 1, which is the case we consider.

On dimensional grounds, the strong coupling energy scale is determined by

$$(E_{strong}^{\zeta\zeta\zeta})^{-3} \sim \Lambda_\zeta(\mathcal{G}_S)^{-3/2} u_S^{-11/2} .$$

Collecting all factors, and omitting factors of order 1, we get

$$E_{strong}^{\zeta\zeta\zeta} \sim \frac{1}{|t|} \left(\frac{g^{1/2} u_S^{11/2}}{|t|^{\mu-1}} \right)^{1/3} . \quad (46)$$

The condition of validity of (semi-)classical approximation, $E_{strong} > |t|^{-1}$, now reads

$$\left(\frac{g u_S^{11}}{|t|^{2(\mu-1)}} \right)^{1/6} > 1 . \quad (47)$$

For small u_S it is stronger than the condition (41), i.e., eq. (47) is valid at later times (smaller $|t|$) than eq. (41).

Let us see whether the condition (47) can be satisfied at the times when the relevant modes of perturbations exit the effective horizon. The most dangerous are the longest modes, i.e., the smallest $k = k_{min}$. To obtain a rough estimate, we take $k_{min} \approx k_*$ (the momentum dependence is weak in view of small $|n_S - 1|$), and relate the exit time (28) at $k = k_*$ with the scalar amplitude (32a). We omit factors of order 1 and obtain

$$t_f^{2(\mu-1)} \sim g \mathcal{A}_\zeta u_S^3 .$$

In this way we find

$$\left(\frac{g u_S^{11}}{|t_f(k_{min})|^{2(\mu-1)}} \right)^{1/6} \sim \left(\frac{u_S^8}{\mathcal{A}_\zeta} \right)^{1/6} \sim \left(\frac{r^{4/\nu}}{\mathcal{A}_\zeta} \right)^{1/6} ,$$

where we make use of eq. (34) with ν given by (33). So, the validity condition (47) for our weak coupling calculations is roughly

$$\left(\frac{r^{4/\nu}}{\mathcal{A}_\zeta} \right)^{1/6} > 1 . \quad (48)$$

We see that there is an interplay between two small numbers, r and \mathcal{A}_ζ . For a crude estimate, we take $\chi \ll 1$ and $\mu \approx 1$, consistent with small $(1 - n_S)$ as given by (31). Then $\nu \approx 3/2$. If we then take, as an example, $r = 0.02$ and insert $\mathcal{A}_\zeta \simeq 2 \cdot 10^{-9}$ into the left hand side of eq. (48), we obtain its numerical value approximately equal to 5, suspiciously close to 1. The lesson we learn from this back-of-envelope estimate is twofold. First, one cannot neglect numerical factors “of order 1” here. In particular, one has to be more precise when evaluating the strong coupling scale E_{strong} : instead of naive dimensional analysis, one has

to consider unitarity bounds. We study this point in general terms in Sec. 2.6 and apply the results to a concrete model in Sec. 3. Second, it is clear that one cannot have arbitrarily small tensor-to-scalar ratio r in our class of models; indeed, $r \simeq 0.02$ appears to be already on the edge of the validity of the weakly coupled description that we make use of. We substantiate the latter observation in Sec. 3 within the concrete model.

The above analysis goes through also in the case $\mu = 1$, $n_S = 1$. Instead of (47), we obtain the condition for the absence of strong coupling, which is again time-independent,

$$(gu_S^{11})^{1/6} > 1. \quad (49)$$

With $\nu = 3/2$ this gives

$$\left(\frac{r^{8/3}}{\mathcal{A}_\zeta}\right)^{1/6} > 1,$$

which is similar to (48). We refine this qualitative argument in Sec. 3.

2.6 Tree level unitarity and strong coupling energy scale

2.6.1 Unitarity relations with different sound speeds

The quantum energy scale of strong coupling is conveniently evaluated by making use of the unitarity bounds on partial wave amplitudes (PWAs) of $2 \rightarrow 2$ scattering [69–72]. In our model we have nine $2 \rightarrow 2$ channels, which we collectively denote by $\alpha\beta$, where $\alpha = (\alpha_1, \alpha_2)$ and $\beta = (\beta_1, \beta_2)$ refer to initial state and final state, respectively:

$$\alpha_1, \alpha_2 \rightarrow \beta_1, \beta_2 = \zeta\zeta \rightarrow \zeta\zeta, \quad (50a)$$

$$\zeta h \rightarrow \zeta\zeta, \quad \zeta\zeta \rightarrow \zeta h \quad (50b)$$

$$\zeta h \rightarrow \zeta h \quad (50c)$$

$$\zeta\zeta \rightarrow hh, \quad hh \rightarrow \zeta\zeta \quad (50d)$$

$$\zeta h \rightarrow hh, \quad hh \rightarrow \zeta h \quad (50e)$$

$$hh \rightarrow hh. \quad (50f)$$

An additional complication is that the perturbations ζ and h have different sound speeds.

In this situation a (fairly obvious) generalization of the PWA unitarity relation is [73]

$$\text{Im } a_{\alpha\beta}^{(l)} = \sum_{\gamma} a_{\alpha\gamma}^{(l)} \frac{g_{\gamma}}{u_{\gamma 1} u_{\gamma 2} (u_{\gamma 1} + u_{\gamma 2})} a_{\gamma\beta}^{(l)*}, \quad (51)$$

where $a_{\alpha\beta}^{(l)}$ is PWA with angular momentum l and initial and final states α and β , respectively, γ refers to two particles in the intermediate state with sound speeds $u_{\gamma 1}$ and $u_{\gamma 2}$, and $g_{\gamma} = 2$

if these intermediate particles are distinguishable and $g_\gamma = 1$ if these particles are identical.³ We omitted contributions to the right hand side due to multiparticle intermediate states, since they can only strengthen the unitarity bound.

Upon redefining

$$\tilde{a}_{\alpha\beta}^{(l)} = \left(\frac{g_\alpha}{u_{\alpha 1} u_{\alpha 2} (u_{\alpha 1} + u_{\alpha 2})} \right)^{1/2} a_{\alpha\beta}^{(l)} \left(\frac{g_\beta}{u_{\beta 1} u_{\beta 2} (u_{\beta 1} + u_{\beta 2})} \right)^{1/2}, \quad (52)$$

we arrive at familiar form of the unitarity relation which we write in the matrix form for the matrix $\tilde{a}_{\alpha\beta}^{(l)}$:

$$\text{Im } \tilde{a}^{(l)} = \tilde{a}^{(l)} \tilde{a}^{(l)\dagger}.$$

The most stringent tree level unitarity bound is obtained for the largest eigenvalue of the tree level matrix $\tilde{a}^{(l)}$ (which is real and symmetric). This bound reads [74]

$$|\text{maximum eigenvalue of } \tilde{a}^{(l)}| \leq \frac{1}{2}.$$

All these properties are derived in detail in Ref. [73].

2.6.2 Dimensional analysis for $u_S \ll 1$.

The model we consider has the large parameter u_S^{-1} which governs small tensor-to-scalar ratio. So, as we have seen, the earliest time after which we can trust our setup depends on u_S . Let us see that the dependence of the rescaled amplitudes $\tilde{a}_{\alpha\beta}^{(l)}$ on u_S is the only source of refinement of the naive estimate for the time t_{cl} of the onset of the classical theory (cf. (41))

$$|t_{cl}|^{2\mu-2} \sim g. \quad (53)$$

We restrict ourselves to the cubic order in perturbations; by experience, higher orders are expected not to give anything new [46, 47]. *Let us ignore the fact that $u_S \ll 1$ for the time being.* Then the entire Lagrangian defined by the functions (15) is proportional to $g(-t)^{-2\mu}$, while the only other ‘‘parameter’’ is t (we ignore constants of order 1). Note that $g(-t)^{-2\mu}$ has dimension (mass)². So, on dimensional grounds, before rescaling to canonically normalized fields, the terms in the cubic Lagrangian have the following schematic form

$$\frac{g}{|t|^{2\mu}} \cdot (|t|\partial)^n \cdot \partial^2 \cdot \varphi^3,$$

where φ stands collectively for (dimensionless) scalar and tensor perturbations, and, with slight abuse of notations, we do not distinguish temporal and spatial derivatives at this stage.

³Equation (51) is not the most general unitarity relation, but it is valid if the right hand side is saturated by the tree level amplitudes. This is sufficient for our purposes.

Going to canonically normalized fields $\varphi^{(c)} \sim (g^{1/2}/|t|^\mu)\varphi$, we write the cubic Lagrangian as follows

$$\frac{|t|^\mu}{g^{1/2}} \cdot (|t|\partial)^n \cdot \partial^2 \cdot \varphi^{(c)3} . \quad (54)$$

With this cubic coupling, its contribution to the $2 \rightarrow 2$ amplitude is, schematically,

$$a^{(l)} \sim \frac{((|t|^\mu/g^{1/2})E^2(E|t|^n)^2)}{E^2} \sim \frac{|t|^{2\mu-2}}{g}(E|t|)^{2n+2} ,$$

where E is the center-of-mass energy, and E^2 in the denominator comes from the propagator, see Fig. 1. This reiterates that ignoring the fact that $u_S \ll 1$, one would obtain the estimate (53) for the time of the onset of the classical theory irrespectively of the channel considered: at that time the amplitude at energy scale $E \sim E_{class} = |t|^{-1}$ saturates the unitarity bound.

Let us now reintroduce $u_S \ll 1$. Importantly, the coefficients in the cubic Lagrangian do not contain inverse powers of u_S , so, no enhancement by u_S^{-1} occurs due to the cubic Lagrangian itself. Note that this is not entirely trivial. First, the theory involves non-dynamical variables α, β, N_i^T entering (13). Their expressions $\alpha(\zeta, h_{ij}), \beta(\zeta, h_{ij})$ and $N_i^T(\zeta, h_{ij})$, obtained by solving the constraint equations, may in principle be enhanced by inverse powers of u_S . As a matter of fact, one can check that this is not the case. Second, one may be tempted to use linearized equations of motion when obtaining the cubic action. This would introduce spurious inverse powers of u_S when inserting $\partial_i \partial_i \zeta = u_S^{-2} \ddot{\zeta}$. The latter subtlety is taken care of by working consistently off-shell, as we do in what follows.

Still, the rescaled amplitudes $\tilde{a}^{(l)}$ acquire the dependence on u_S . Schematically, the rescaled amplitudes are now

$$\tilde{a}^{(l)} \sim \frac{|t|^{2\mu-2}}{g}(E|t|)^{2n+2}u_S^{-K} ,$$

where K depends on the process. Now the time of the onset of the classical theory is determined by

$$|t_{cl}|^{2\mu-2} \sim gu_S^K .$$

The larger K , the smaller $|t_{cl}|$, the later the system enters the classical theory/weak coupling regime. So, to figure out the actual time t_{cl} (the latest of the “strong coupling times”), we are going to hunt for processes whose rescaled amplitudes are enhanced by u_S^{-K} with the largest value of K .

In the case $\mu = 1$, the validity condition for (semi-)classical treatment is $gu_S^K > 1$, so, again, the strongest bound on the parameters of a model is obtained for the largest value of K .

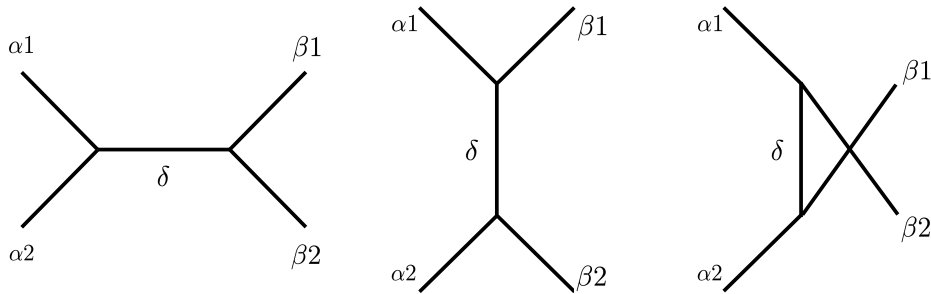


Figure 1: Tree-level diagrams. Particles α_1 , α_2 , β_1 , β_2 and δ can be scalar or tensor.

2.6.3 Hierarchy of rescaled amplitudes

Let us consider tree-level diagrams of the types shown in Fig. 1.

In our class of models, the amplitudes $\tilde{a}_{\alpha\beta}^{(l)}$ with one and the same energy E in the center-of-mass frame $\mathbf{p}_{\alpha_1} = -\mathbf{p}_{\alpha_2}$ and different particles in the initial, final and intermediate states show hierarchical pattern in terms of the large parameter u_S^{-1} . This pattern is due to the following properties:

(i) Due solely to rescaling, the rescaled amplitudes (52) are enhanced by a factor $u_S^{-3/2}$ for two initial (or two final) *scalar* external legs; by a factor $u_S^{-1/2}$ if initial (or final) legs are ζh ; no enhancement of this sort is associated with two tensor initial (or final) external legs.

(ii) Since the energy and momentum of a *scalar* are related by $\omega = u_S p$ (we reserve the notation E for the center-of-mass energy), spatial momentum of an incoming or outgoing scalar may be either of order $p \sim E/u_S$ or of order $p \sim E$. In the former case (only!) every *spatial* derivative in a vertex, that acts on external leg ζ gives enhancement u_S^{-1} . The same observation applies to internal line ζ in t - and u -channels, if spatial momentum transfer is of order E/u_S .

(iii) The scalar propagator is given by

$$S(\omega, p) = \frac{1}{\omega^2 - u_S^2 p^2}.$$

For $\omega = 0$ (t - and/or u -channel diagrams with internal line ζ) this gives enhancement u_S^{-2} , provided that the momentum transfer is $p \sim E$ (but not E/u_S).

To proceed further, we note that the maximum number of *spatial* derivatives in triple- ζ vertex is 4. In the particular class of Horndeski models (7) with $G_5 = 0$, and, furthermore, with $G_4 = G_4(\phi)$, there are at most 2 *spatial* derivatives in other vertices. We discuss this point in Appendix C. Another useful observation is that for a given center-of-mass energy E , incoming (outgoing) momenta are of order $p \sim E/u_S$ if *both* initial (final) particles are ζ , and $p \sim E$ otherwise.

We now consider various channels and diagrams separately.

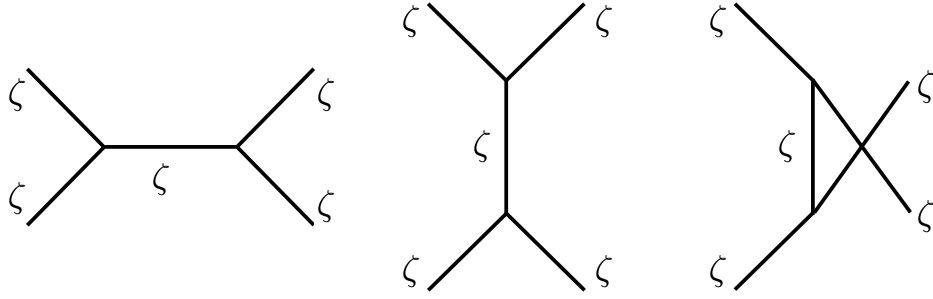


Figure 2: Purely scalar tree-level diagrams: case **(a)**.

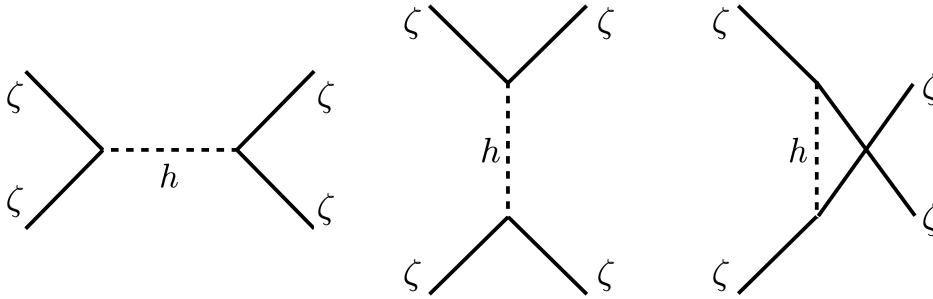


Figure 3: Tree-level diagrams with ζ -legs and h -propagators: case **(b)**.

(a). Purely scalar diagrams, Fig. 2, process (50a). In this case all spatial momenta, including intermediate momentum in t - and u -channel diagrams, are of order E/u_S . Hence, the enhancement mechanisms (i) and (ii) are at work, while the mechanism (iii) is not. The maximum number of spatial derivatives at each vertex is 4, so the diagrams are of order

$$u_S^{-3/2} \cdot u_S^{-3/2} \cdot 1 \cdot u_S^{-4} \cdot u_S^{-4} = u_S^{-11},$$

(hereafter the first two factors are due to enhancement (i), the third factor due to enhancement (iii) and the last two factors due to enhancement (ii)). This precisely matches the amplitude that one obtains from the cubic action (45).

(b). Strong enhancement would appear to occur also for diagrams with scalar external legs and tensor exchange, Fig. 3. However, as we pointed out, the maximum number of spatial derivatives in each $\zeta\zeta h$ vertex is 2 (rather than 4). Therefore, the enhancement factor is

$$u_S^{-3/2} \cdot u_S^{-3/2} \cdot 1 \cdot u_S^{-2} \cdot u_S^{-2} = u_S^{-7}. \quad (55)$$

So, tensor exchange gives subdominant contribution.

(c). Process (50b) with t -channel ζ -exchange, Fig. 4, left diagram. The incoming spatial momenta are of order E , while outgoing ones are of order E/u_S . So, the spatial momentum

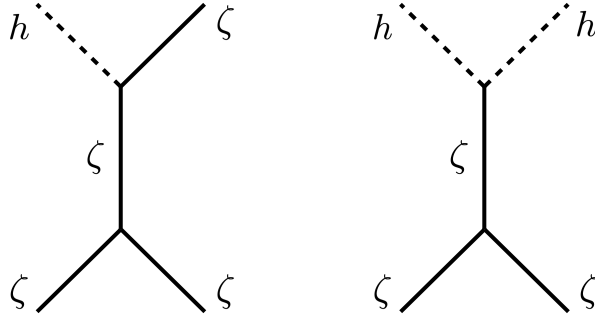


Figure 4: Tree-level t-channel diagrams: cases **(c)** (left) and **(d)** (right).

transfer is of order E/u_S and the mechanism (iii) does not work. The enhancement factor is

$$u_S^{-1/2} \cdot u_S^{-3/2} \cdot 1 \cdot u_S^{-2} \cdot u_S^{-4} = u_S^{-8} , \quad (56)$$

so this process is also subdominant.

(d). To illustrate the mechanism (iii), we consider the process (50d) with t -channel ζ -exchange, Fig. 4, right diagram. Spatial momenta of incoming and outgoing particles are of order $p \sim E$, the spatial momentum transfer is also of order E , so the mechanism (ii) does not work. We find the enhancement factor

$$u_S^{-1/2} \cdot u_S^{-1/2} \cdot u_S^{-2} \cdot 1 \cdot 1 = u_S^{-3} , \quad (57)$$

which is again weak.

Other diagrams can be studied in a similar way, and all of them are suppressed as compared to purely scalar process **(a)**. The general argument is straightforward. By replacing one or more external scalar legs in a purely scalar diagram of the case **(a)** by tensor leg(s), one loses at least an enhancement factor u_S^{-1} from (i) and another factor u_S^{-2} from (ii). One could in principle gain a factor u_S^{-2} due to (iii) (we have seen in our example **(c)** that this is actually not the case if one replaces just one scalar leg), but in any case, the overall suppression of a new diagram is at least u_S as compared to the original, purely scalar one⁴. Replacing the scalar internal line by the tensor line does not improve the situation, and in the particular case **(b)** produces suppressed result.

We conclude that the latest time of the onset of the classical theory t_{cl} is associated with the scalar sector of the theory. This means, in particular, that the search for the largest eigenvalue of the rescaled PWA matrix \tilde{a} (Sec. 2.6.1) is unnecessary. The relevant terms in

⁴In reality the suppression is always even stronger, cf. (55), (56), (57). Moreover, in mixed sectors some couplings in the cubic action are themselves suppressed by positive powers of u_S , leading to even stronger suppression of the contributions to the amplitudes.

the cubic scalar action are those with four *spatial* derivatives. Modulo numerical factors, the time t_{cl} is indeed determined from (47),

$$|t_{cl}|^{2\mu-2} \sim g u_S^{11},$$

whereas for $\mu = 1$ the condition is $g u_S^{11} > 1$. To refine these estimates, we perform the calculation of the dominant partial wave amplitudes in the scalar sector.

2.6.4 Strong coupling scale from tree-level unitarity

We are now ready to perform the calculation of the strong coupling energy scale, as implied by the tree-level unitarity bound. The (off-shell) cubic action with 4 spatial derivatives in the scalar sector is given by (42). We continue to use the approach of Sec. 2.6.3, set $a = 1$ as before and work with the field $\tilde{\zeta} = (2\mathcal{G}_S)^{-1/2}\zeta$, which has canonical time-derivative term and gradient term with sound speed u_S . Then the cubic action reads

$$\mathcal{S}_{\zeta\zeta\zeta}^{(3)} = \int dt d^3x \tilde{\Lambda}_\zeta \partial^2 \tilde{\zeta} (\partial \tilde{\zeta})^2,$$

where

$$\tilde{\Lambda}_\zeta = (2\mathcal{G}_S)^{-3/2} \Lambda_\zeta = \frac{\lambda_\zeta |t|^\mu}{g_S^{3/2} g^{1/2}} \cdot |t|^2.$$

It is now straightforward to calculate the $2 \rightarrow 2$ matrix element $M(\cos\theta, E)$ as function of scattering angle θ and center-of-mass energy E . We get

$$M = \frac{E^6}{4u_S^8} (1 - \cos^2\theta) \tilde{\Lambda}_\zeta^2,$$

(the origin of the dependence on u_S is the mechanism (ii) in Sec. 2.6.3). We now write the rescaled PWA amplitude

$$\tilde{a}^{(l)} = \frac{1}{2u_S^3} \cdot \frac{1}{32\pi} \int d(\cos\theta) P_l(\cos\theta) M,$$

where P_l are Legendre polynomials, the factor $(2u_S^3)^{-1}$ comes from the redefinition (52) (i.e., it is due to the mechanism (i) in Sec. 2.6.3), and obtain

$$\begin{aligned} \tilde{a}^{(0)} &= \frac{\tilde{\Lambda}_\zeta^2 E^6}{192\pi u_S^{11}}, \\ \tilde{a}^{(2)} &= -\frac{\tilde{\Lambda}_\zeta^2 E^6}{960\pi u_S^{11}}. \end{aligned}$$

The lowest bound on the energy of strong coupling comes from the s -wave amplitude. It saturates the unitarity bound $|\tilde{a}^{(0)}| \leq 1/2$ at energy

$$E_{strong}(t) = \left(\frac{96\pi u_S^{11}}{\tilde{\Lambda}^2} \right)^{1/6} = \frac{(96\pi)^{1/6}}{|t|} \left(\frac{g_S^3 g u_S^{11}}{\lambda_\zeta^2 |t|^{2\mu-2}} \right)^{1/6}.$$

This refines the estimate (46). Proceeding as in Sec. 2.5, we calculate the ratio of quantum and classical energy scales at the time when the mode $k_* \approx k_{min}$ exits the effective horizon:

$$\frac{E_{strong}(t_f(k_*))}{E_{class}(t_f(k_*))} \equiv \frac{E_{strong}(k_*)}{E_{class}(k_*)} = E_{strong}(t_f(k_*)) \cdot |t_f(k_*)| = C \cdot \left(\frac{u_S^8}{\mathcal{A}_\zeta} \right)^{1/6}, \quad (59)$$

where

$$C = \frac{96^{1/6} g_S^{1/3}}{|\lambda_\zeta|^{1/3}} \left(\frac{2^{2\frac{\mu-1}{1-\chi}} (1-\chi)^{2\frac{\mu-\chi}{1-\chi}} (2\mu-3\chi)^{2\frac{1-\mu}{1-\chi}}}{\Gamma^2(1-\nu) \sin^2(\nu\pi)} \right)^{1/6}. \quad (60)$$

This is the desired result for general models from the class (15). In the case $\mu = 1$, $n_S = 1$ (and hence $\nu = 3/2$) we have

$$C = \frac{96^{1/6} g_S^{1/3}}{|\lambda_\zeta|^{1/3}} \left(\frac{(1-\chi)^2}{4\pi} \right)^{1/6}.$$

The result (59) depends in a fairly complicated way, through the parameters χ , g_S and λ_ζ , on both the form of the Lagrangian functions ($a_2(N)$ and $a_3(N)$ in (15)) and the solution to the equations of motion, eqs. (18). To get an idea of how restrictive the condition for the absence of strong coupling at the horizon exit is, we now turn to concrete examples where all above points are seen explicitly.

3 Examples

3.1 $\mu > 1$, $n_S < 1$.

In this Section we consider a particular model of the type (15) with the simple forms of the Lagrangian functions:

$$a_2(N) = c_2 + \frac{d_2}{N}, \quad (61a)$$

$$a_3(N) = c_3 + \frac{d_3}{N}, \quad (61b)$$

where c_2 , c_3 , d_2 , d_3 , are dimensionless constants. Making use of eqs. (23), we obtain

$$f_S = -2 \left(\frac{4\mu - 2 + d_3}{2\chi + d_3} \right),$$

$$g_S = \frac{6d_3^2}{(2\chi + d_3)^2}.$$

In accordance with our discussion in Sec. 2.3, one finds that the only way to obtain small tensor-to-scalar ratio (34) is to ensure that $f_S \ll 1$ and $g_S \sim 1$, so that $u_S^2 = f_S/g_S \ll 1$. We begin with the case $\mu > 1$, which corresponds to $n_S < 1$ in accordance with the Λ CDM value (6), and ensure the small value of u_S by imposing a *fine tuning relation*

$$d_3 = -2 .$$

This choice appears rather remarkable, but we do not know whether it may be a consequence of some symmetry or dynamical principle. Anyway, with this choice, we have

$$f_S = \frac{4(\mu - 1)}{1 - \chi} = 2(1 - n_S) ,$$

$$g_S = \frac{6}{(1 - \chi)^2} ,$$

where we recall eq. (31). Interestingly, small tensor-to-scalar ratio $r \sim f_S^\nu/g_S^{\nu-1}$ and small scalar tilt $(1 - n_S)$ are now governed by one and the same small parameter $(\mu - 1)$.

Proceeding with $d_3 = -2$, we find that equations for the background have relatively simple form. These are algebraic equations:

$$3\chi^2 - 6\chi + c_2 N^2 = 0 ,$$

$$3\chi^2 + 2(2\mu + 1)(1 - \chi) - \kappa N + c_2 N^2 = 0 ,$$

where

$$\kappa = c_3(1 + 2\mu) - d_2 . \tag{65}$$

The relevant solution to these equations is (the second solution does not yield stable bounce)

$$\chi = \frac{3 + 8\rho(\mu - 1)(2\mu + 1) - \sqrt{9 - 12\rho(2\mu + 1)(5 - 2\mu)}}{3 + 16\rho(\mu - 1)^2} , \tag{66a}$$

$$N = \frac{2}{\kappa} [1 + 2\mu - 2(\mu - 1)\chi] , \tag{66b}$$

where

$$\rho = \frac{c_2}{\kappa^2} . \tag{67}$$

While the expression for N is not of particular physical significance (the only requirement is that $N > 0$), the value of χ is an important characteristic of the solution. Note that while N depends on c_2 and κ separately, the parameter χ depends (for given μ) on one combination ρ out of the three Lagrangian parameters remaining after setting $d_3 = -2$. We will see in what follows that μ and ρ (or, equivalently, χ) are the only parameters relevant also for the strong coupling issue.

For small and positive $(\mu - 1)$, the allowed range of parameters is

$$\kappa > 0, \quad 0 < \rho \lesssim \frac{2}{27}. \quad (68)$$

These relations ensure that $N > 0$ and, importantly, $2\mu - 3\chi > 0$, see (27).

We are now equipped with the explicit formulas to see what range of the tensor-to-scalar ratio is consistent with our weak coupling calculations. We obtain from (43), (44)

$$\theta = 1 - \chi, \quad (69a)$$

$$\lambda_\zeta = \frac{1}{4(1 - \chi)^2}, \quad (69b)$$

while the parameter ν is still given by (33). Besides the dependence on μ , these parameters again depend on ρ only.

We express the parameter μ through n_S and χ using (31). Then we are left with the only free parameter χ (or, equivalently, ρ). Our final formulas are obtained from (34) and (59):

$$r = 48(1 - \chi)^{2(\nu-1)} \left(\frac{1 - n_S}{3} \right)^\nu,$$

$$\frac{E_{strong}(k_*)}{E_{class}(k_*)} = E_{strong}(t_f(k_*)) \cdot |t_f(k_*)| = \tilde{C} \cdot \left(\frac{r^{4/\nu}}{\mathcal{A}_\zeta} \right)^{1/6},$$

where, as before, $\nu = 2 - n_S/2$ and

$$\tilde{C} = \frac{C}{(8g_S)^{2/3\nu}},$$

where C is given by (60), so that

$$\tilde{C} = 2^{\frac{12-11n_S}{24-6n_S}} 3^{\frac{4-3n_S}{24-6n_S}} (1 - \chi)^{\frac{12-n_S}{3(4-n_S)}} \left(\frac{(2 - 2\chi)^{1-n_S} \left(2 + (1 - n_S) - \chi(3 + (1 - n_S)) \right)^{-(1-n_S)}}{\Gamma^2\left(\frac{n_S}{2} - 1\right) \sin^2 \left[\left(2 - \frac{n_S}{2}\right)\pi \right]} \right)^{1/6}$$

$$\approx \frac{3^{1/18} (1 - \chi)^{11/9}}{2^{5/18} \pi^{1/6}} = 0.7 \cdot (1 - \chi)^{11/9},$$

where we set $n_S = 1$ in the last two expressions. In Fig. 5 we show r -ratio and the ratio $E_{strong}(k_*)/E_{cl}(k_*)$ as functions of χ for the Λ CDM central value $n_S = 0.9649$ suggested by observations. The main message is that the value of r is bounded from below in our model, $r > 0.018$ for $n_S = 0.9649$, even for very generous unitarity bound $E_{strong}(k_*)/E_{cl}(k_*) > 1$. Note that the parameters should obey $(2\mu - 3\chi) > 0$ which translates to

$$\chi < \frac{3 - n_S}{4 - n_S} \approx \frac{2}{3}. \quad (70)$$

This bound is also shown in Fig. 5.

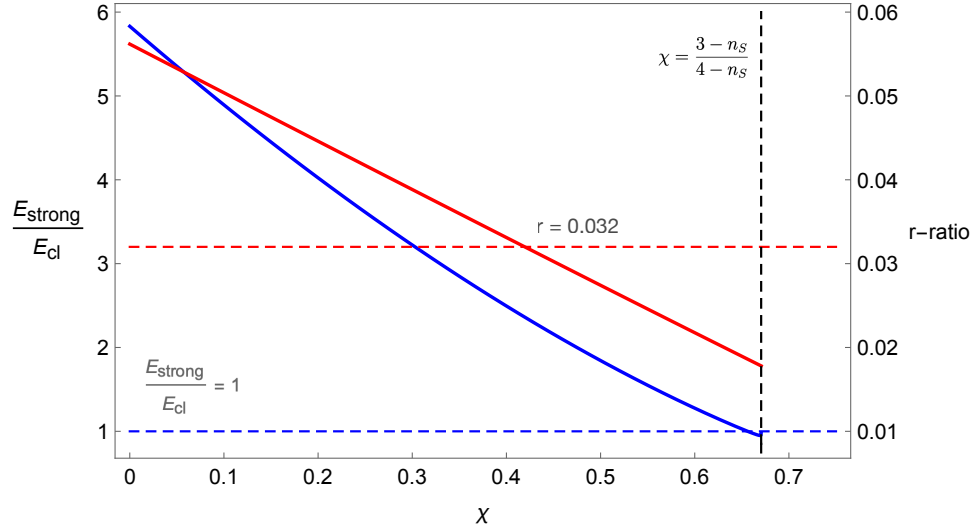


Figure 5: The ratio $E_{strong}(k_*)/E_{cl}(k_*)$ (blue line) and r -ratio (red line) as functions of χ for the central value $n_s = 0.9649$. The allowed range $r < 0.032$ and the unitarity bound $E_{strong}(k_*)/E_{cl}(k_*) > 1$ restrict the parameter space to the right lower part.

In Fig. 6 we show what happens if the scalar tilt n_s is varied within the observationally allowed range. A point to note is that in the entire allowed range, the parameter r is fairly large, $r > 0.015$, while the strong coupling scale is always close to the classical energy scale, $E_{strong} \lesssim 3E_{cl}$. We conclude that our simple model is on the verge of being ruled out.

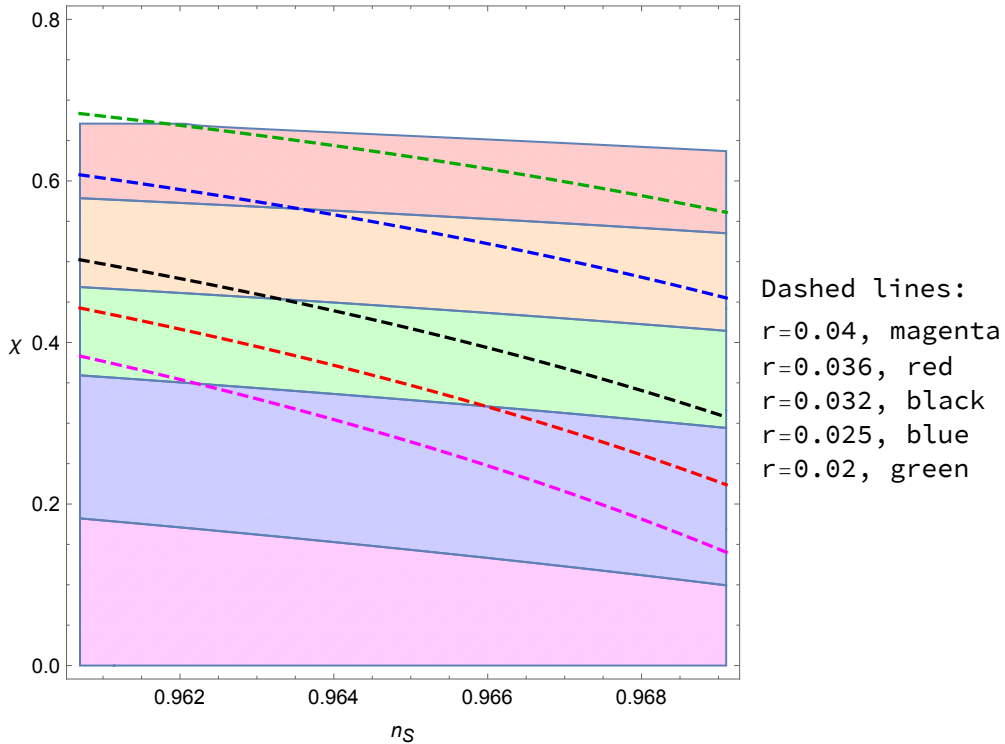


Figure 6: Space of parameters n_S and χ . Colored strips correspond to different ratios of strong coupling scale to classical scale: $1 < E_{strong}(k_*)/E_{cl}(k_*) < 1.5$ (red), $1.5 < E_{strong}(k_*)/E_{cl}(k_*) < 2.2$ (orange), $2.2 < E_{strong}(k_*)/E_{cl}(k_*) < 3$ (green), $3 < E_{strong}(k_*)/E_{cl}(k_*) < 4.5$ (blue), $4.5 < E_{strong}(k_*)/E_{cl}(k_*)$ (magenta). Dashed lines show the tensor-to-scalar ratio: $r = 0.02$ (green), $r = 0.025$ (blue), $r = 0.032$ (black), $r = 0.036$ (red), and $r = 0.04$ (magenta).

Choosing appropriate values of (χ, n_S) one immediately obtains concrete form of scale factor (17) and Hubble parameter $H = \chi/t$ in Jordan frame for the contraction stage. For example, $a(t)/d$ and H for $\chi = 0.4$, $n_S = 0.967$, (and i.e. for $\mu = 1.0099$) are shown in Fig. 7. It is also interesting to find corresponding scale factor and Hubble parameter in Einstein frame. The scale factor $a_E(t_E)$ (t_E is a cosmic time in Einstein frame) is given by (5), while Hubble parameter in Einstein frame is

$$H_E \equiv \frac{1}{a_E} \frac{da_E}{dt_E} = \left(\frac{\mu - \chi}{\mu - 1} \right) \frac{1}{t_E}.$$

These scale factor and Hubble parameter with $\chi = 0.4$ and $n_S = 0.967$ ($\mu = 1.0099$) in Einstein frame are shown in Fig. 8.

Finally, in Appendix F we present an explicit numerical example of stable and subluminal evolution where the contraction from this section terminates and expansion begins (bounce),

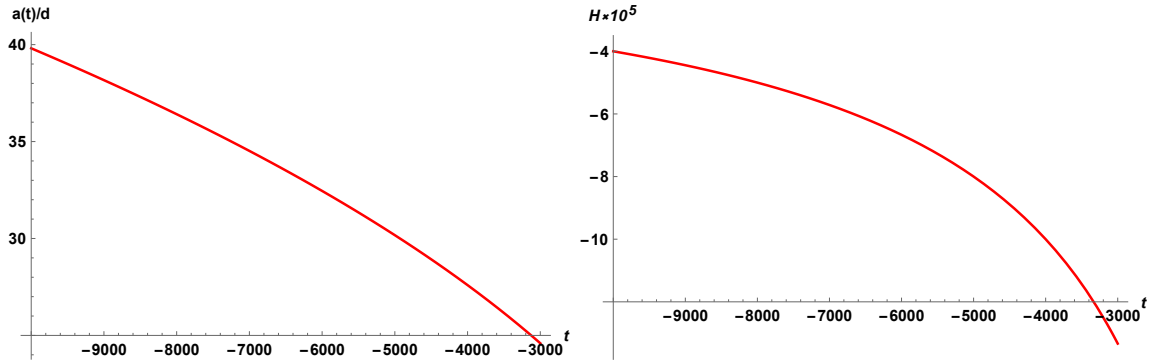


Figure 7: The scale factor $a(t)$ divided by d (left panel) and the Hubble parameter $H(t)$ (right panel) in Jordan frame in the model with $\chi = 0.4$, $n_S = 0.967$ (and $\mu = 1.0099$).

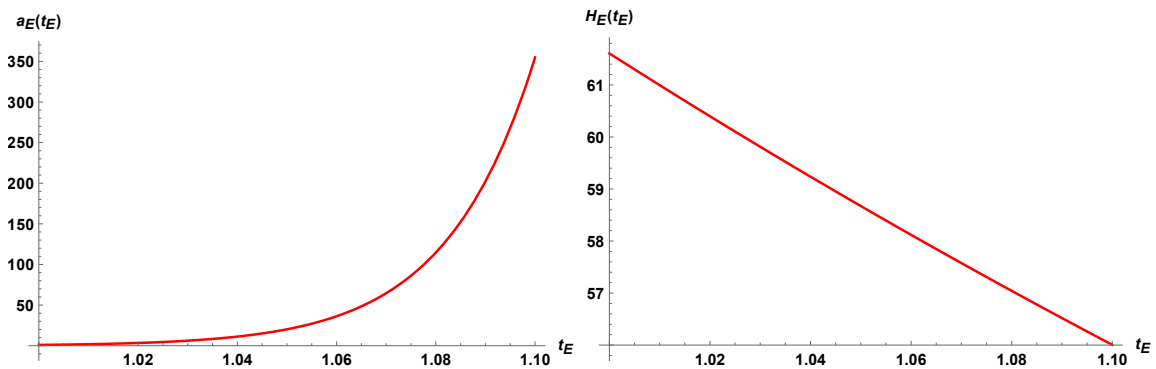


Figure 8: The scale factor $a_E(t_E)$ (left panel) and the Hubble parameter $H_E(t_E)$ (right panel) in Einstein frame in the model with $\chi = 0.4$, $n_S = 0.967$ (and $\mu = 1.0099$).

then the Universe turns into the kination epoch at future times. In this model, the Einstein-Hilbert action for gravity is restored during the kination epoch and thus all background quantities such as the energy scales, the Hubble parameter can be calculated in a usual way. Similar procedure was done in Ref. [47], where different models of bouncing Universe and genesis turn into general relativity with a conventional massless scalar field that drives the expansion in the future, at large positive times. The kination epoch is assumed to end up with reheating through, for example, one of the mechanisms of Refs. [75, 76]. We also prove for our concrete numerical example (in the same Appendix F), that the proposed evolution is physically relevant, since around 60 e-folds of contraction can be accommodated so the wavelength of primordial fluctuations stretches ~ 60 Hubble scales at the end of the contracting phase and before the Universe bounces.

3.2 $\mu = 1, n_S = 1$

We now consider the case $\mu = 1, n_S = 1$ consistent with the early dark energy idea [51, 52]. Our model is still defined by the functions (61), now with $\mu = 1$. Unlike in Sec. 3.1, we ensure that $f_S \ll 1$, and hence the scalar sound speed is small, by choosing

$$d_3 = -2 + \epsilon, \quad \epsilon \ll 1.$$

Then

$$f_S = \frac{2\epsilon}{2 - 2\chi - \epsilon},$$

$$g_S = \frac{6(2 - \epsilon)^2}{(2 - 2\chi - \epsilon)^2},$$

while θ and λ_ζ are still given by (69). Note that $\epsilon > 0$, since we require $f_S > 0$.

Background equations of motion are again algebraic, and their solution is

$$\chi = \frac{(2 - \epsilon) \left(1 + 6\epsilon\rho - \sqrt{1 - 12(1 - \epsilon)\rho} \right)}{2(1 + 3\epsilon^2\rho)},$$

$$N = \frac{3(2 - \epsilon) \left(2 - \epsilon(1 - \sqrt{1 - 12(1 - \epsilon)\rho}) \right)}{2\kappa(1 + 3\epsilon^2\rho)},$$

with $\kappa = 3c_3 - d_2$, $\rho = c_2/\kappa^2$. For given ϵ , we can again trade the parameter ρ for χ , hence the two relevant parameters are now χ and ϵ . Having all formulas above, we are ready to understand what range of the r -ratio is consistent with the weak coupling regime. We recall (34) and (59), set $\nu = 3/2$ and find

$$r = \frac{16\epsilon^{3/2}}{[3(2 - 2\chi - \epsilon)]^{1/2}(2 - \epsilon)},$$

$$\frac{E_{strong}}{E_{class}} = \tilde{B} \cdot \left(\frac{r^{8/3}}{\mathcal{A}_\zeta} \right)^{1/6},$$

where the coefficient \tilde{B} is

$$\tilde{B} = 6^{1/18}(1 - \chi) \left(\frac{[\frac{2-2\chi-\epsilon}{2-\epsilon}]^{4/3}}{4\pi} \right)^{1/6} = 0.7 \cdot (1 - \chi) \left(\frac{2 - 2\chi - \epsilon}{2 - \epsilon} \right)^{2/9}.$$

In Fig. 9 we show $\frac{E_{strong}}{E_{class}}$ and r on the plane of the two parameters ϵ and χ . One observes that in the model with $\mu = 1$ it is easier to obtain small tensor-to-scalar ratio, still insisting on the generation of the perturbations in the weak coupling regime. Nevertheless, the value

of r cannot be much smaller than 0.01, otherwise one would face with the strong coupling problem.

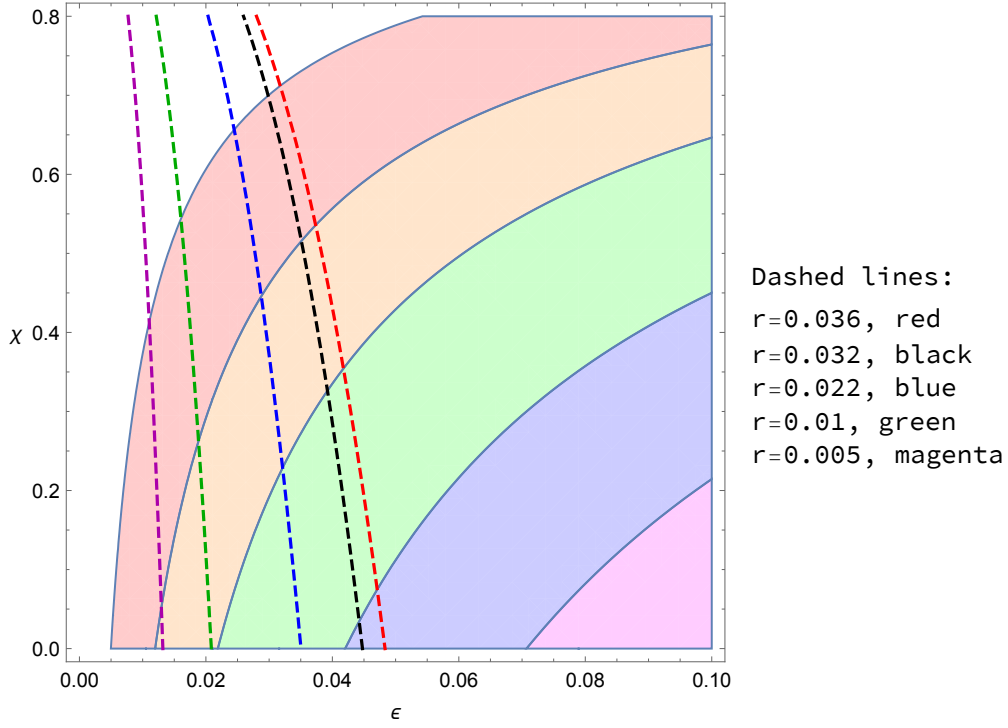


Figure 9: Space of parameters ϵ and χ in the case $\mu = 1$. Colored strips correspond to different ratios of strong coupling scale to classical scale: $1 < E_{strong}/E_{cl} < 1.8$ (red), $1.8 < E_{strong}/E_{cl} < 2.7$ (orange), $2.7 < E_{strong}/E_{cl} < 4.2$ (green), $4.2 < E_{strong}/E_{cl} < 6$ (blue), $6 < E_{strong}/E_{cl}$ (magenta). Dashed lines show the tensor-to-scalar ratio: $r = 0.005$ (magenta), $r = 0.01$ (green), $r = 0.022$ (blue), $r = 0.032$ (black), and $r = 0.036$ (red).

Finally, choosing appropriate value of χ in this case one can easily find the form of scale factor (17) and Hubble parameter $H = \chi/t$ in Jordan frame. For example, $a(t)/d$ and H for $\chi = 0.1$ are shown in Fig. 10.

Here we give scale factor and Hubble parameter in Einstein frame as well

$$a_E = \frac{g_1}{(1-\chi)} d^{1/\chi} e^{(1-\chi)\frac{t_E}{g_1}},$$

$$H_E = \frac{da_E}{a_E dt_E} = \frac{1-\chi}{g_1},$$

with $g_1 \equiv \frac{\sqrt{g}}{M_{Pl}}$ and t_E is a cosmic time in Einstein frame. We discuss all related calculations of these scale factor and Hubble parameter in Einstein frame in Appendix E. Scale factor (divided by some convenient constant) in Einstein frame with chosen $\chi = 0.1$ is shown in Fig. 11.

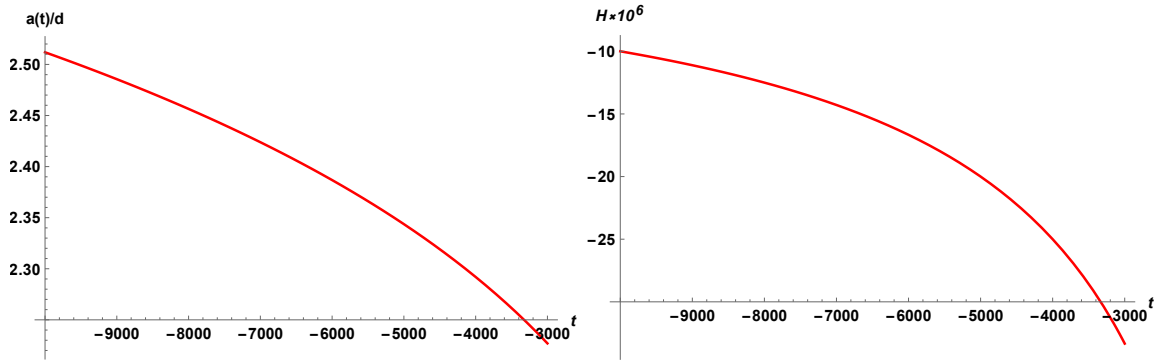


Figure 10: The scale factor $a(t)$ divided by d (left panel) and the Hubble parameter $H(t)$ (right panel) in Jordan frame in the model with $\chi = 0.1$, $n_S = 1$, and $\mu = 1$.

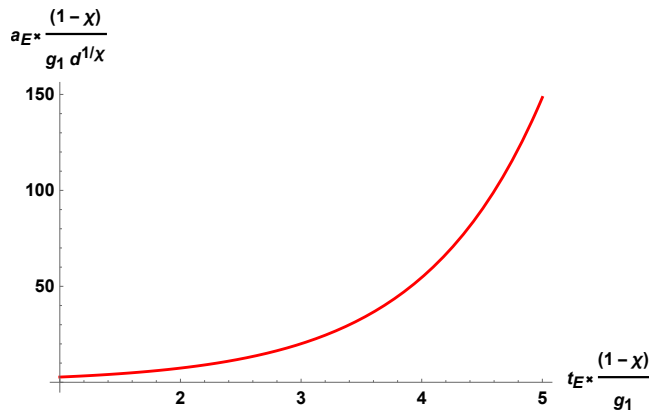


Figure 11: The scale factor $a_E(t_E)$ (multiplied by some convenient constant) in Einstein frame in the model with $\chi = 0.1$, $n_S = 1$, and $\mu = 1$.

4 Conclusion

In this paper we have studied, in the framework of the Horndeski theory, the contracting cosmological stage which can afterwards pass through bounce to a realistic cosmological expansion, as discussed in detail, e.g., in Ref. [47]. We have found that this stage is capable of producing experimentally consistent scalar power spectrum and small enough tensor-to-scalar ratio r . Small value of $(1 - n_S)$ is obtained at the expense of mild fine tuning, while small r requires small scalar sound speed, $r \sim u_S^3$. The latter property is in potential tension with the requirement of weak coupling at the time of the generation of scalar perturbations: small u_S enhances the scattering amplitudes and modifies the unitarity relation, which is violated at energies dangerously close to the energy scale of the classical evolution. Thus, very small values of r are strongly disfavored in our class of models. We have illustrated these properties in very concrete examples within the Horndeski theory.

While our motivation originates from the interest in constructing complete, singularity-free cosmologies, our initial stage of the bounce is conformally equivalent to rapidly expanding Universe, and, indeed, the red scalar tilt is obtained in a model, conformally equivalent⁵ to G -inflation [5]. So, we expect that our observation of the importance of the quantum strong coupling problem may be relevant to the models of G -inflation, and possibly also k -inflation. We think this line of thought is worth pursuing in the future.

Finally, it is known, that models of galileon genesis and k -inflation typically produce non-gaussian features incompatible with current observations of the CMB. It would be interesting to examine this problem for the contracting models, one of which was studied in this paper. We plan to turn to this issue in the upcoming works.

Acknowledgements

The authors are grateful to M. Shaposhnikov, A. Starobinsky, A. Westphal, and C. Wetterich for helpful discussions and Yun-Song Piao for useful correspondence. This work has been supported by Russian Science Foundation Grant No. 19-12-00393.

Appendix A. General expressions in the Horndeski model

Here we give explicit formulas for a theory with action (8). Equations of motion for spatially flat FLRW background read [77]

$$(NA_2)_N + 3NA_3NH + 6N^2(N^{-1}A_4)_NH^2 = 0, \quad (71a)$$

$$A_2 - 6A_4H^2 - \frac{1}{N} \frac{d}{dt} (A_3 + 4A_4H) = 0, \quad (71b)$$

where $H = (Na)^{-1}(da/d\hat{t})$ is the Hubble parameter. The coefficient functions in the quadratic actions for perturbations (14) are given by [29]

$$\mathcal{G}_T = -2A_4, \quad (72a)$$

$$\mathcal{F}_T = 2B_4, \quad (72b)$$

and

$$\mathcal{F}_S = \frac{1}{aN} \frac{d}{dt} \left(\frac{a}{\Theta} \mathcal{G}_T^2 \right) - \mathcal{F}_T, \quad (73a)$$

$$\mathcal{G}_S = \frac{\Sigma}{\Theta^2} \mathcal{G}_T^2 + 3\mathcal{G}_T, \quad (73b)$$

⁵The action for our set of models has fairly simple form in our Jordan frame and is a lot more contrived in the inflationary Einstein frame. For this reason we have performed our analysis entirely in the Jordan frame.

with

$$\Sigma = NA_{2N} + \frac{1}{2}N^2A_{2NN} + \frac{3}{2}N^2A_{3NN}H + 3(2A_4 - 2NA_{4N} + N^2A_{4NN})H^2, \quad (74a)$$

$$\Theta = 2H\left(\frac{NA_{3N}}{4H} - A_4 + NA_{4N}\right). \quad (74b)$$

Appendix B. Power spectra

In this Appendix we present, for completeness, the calculation of the power spectra of perturbations. The quadratic actions for perturbations are given by eqs. (19), where the scale factor is written in eq. (17) and the coefficients are given by eqs. (20), (22).

We give the calculation for the scalar perturbations; tensor perturbations are treated in the same way. We introduce the canonically normalized field ψ via

$$\zeta = \frac{1}{(2\mathcal{G}_S a^3)^{1/2}} \cdot \psi,$$

so that the quadratic action is

$$\mathcal{S}_{\psi\psi}^{(2)} = \int d^3x dt \left[\frac{1}{2}\dot{\psi}^2 + \frac{1}{2}\frac{\ddot{\alpha}}{\alpha}\psi^2 - \frac{u_S^2}{2a^2}(\vec{\nabla}\psi)^2 \right],$$

where

$$\alpha = (2\mathcal{G}_S a^3)^{1/2} = \frac{\text{const}}{(-t)^{\frac{2\mu-3\chi}{2}}}.$$

Once the inequality (27) is satisfied, the second term in the integrand is negligible at early times $t \rightarrow -\infty$, and the field ψ can be treated within the WKB approximation. The properly normalized negative-frequency WKB solution is

$$\psi_{WKB} = \frac{1}{(2\pi)^{3/2}} \frac{1}{\sqrt{2\omega}} \cdot e^{-i\int\omega dt} = \frac{1}{(2\pi)^{3/2}} \sqrt{\frac{d}{2u_S k}} (-t)^{\chi/2} \cdot e^{i\frac{u_S}{d} \frac{k}{1-\chi} (-t)^{1-\chi}},$$

where

$$\omega = \frac{u_S k}{a} = \frac{u_S \cdot k}{d(-t)^\chi},$$

We now solve the complete equation (26) for perturbation ζ with the early time asymptotics $\zeta \rightarrow \zeta_{WKB} = (2\mathcal{G}_S a^3)^{-1/2} \psi_{WKB}$ and obtain

$$\zeta = \mathfrak{C} \cdot (-t)^\delta \cdot H_\nu^{(1)}(\beta(-t)^{1-\chi}),$$

where

$$\begin{aligned}\delta &= \frac{1 + 2\mu - 3\chi}{2}, \\ \beta &= \frac{u_S k}{d(1 - \chi)}, \\ \nu &= \frac{\delta}{\gamma} = \frac{1 + 2\mu - 3\chi}{2(1 - \chi)},\end{aligned}$$

and normalization factor \mathfrak{C} is found by matching to the WKB solution; modulo an irrelevant time-independent phase, we have

$$\mathfrak{C} = \frac{1}{(gg_S)^{1/2}} \frac{1}{2^{5/2}\pi(1 - \chi)^{1/2}} \frac{1}{d^{3/2}}.$$

At late times (formally, $|t| \rightarrow 0$), this solution is time-independent,

$$\zeta = (-i) \frac{\mathfrak{C}}{\sin(\nu\pi)} \frac{(1 - \chi)^\nu}{u_S^\nu \Gamma(1 - \nu)} \left(\frac{2d}{k}\right)^\nu.$$

It determines the scalar power spectrum via

$$\mathcal{P}_\zeta = 4\pi k^3 \zeta^2.$$

Collecting all factors, we obtain the result quoted in (30).

Tensor power spectrum is obtained by replacing $2\mathcal{G}_S \rightarrow \mathcal{G}_T/4$ (i.e., $g_S \rightarrow 1/4$) and $u_S \rightarrow u_T = 1$, and multiplying by 2 due to two tensor polarizations. This gives the result for \mathcal{P}_T quoted in (30).

Appendix C. Largest terms in cubic actions

In this Appendix we collect the expressions for cubic actions that contain the largest number of *spatial* derivatives. As we discuss in the main text, we consistently work off-shell, i.e., do not use equations of motion for dynamical perturbations ζ , h_{ij} when evaluating the unconstrained cubic action. Neither we employ field redefinitions to get rid of the terms in the cubic action which are proportional to the linearized field equations; we only use the background equations of motion and perform integrations by parts. This is precisely what is done in Refs. [45, 65, 66]. In this approach, no coefficients in the cubic action are enhanced by inverse powers of u_S . The terms with the largest number of spatial derivatives are readily extracted from Ref. [45]. We stick to the action (7) with $G_5 = 0$, or, equivalently, the action (8); furthermore, in our set of models we have $G_4 = G_4(\phi)$, or, equivalently,

$$A_4 = -B_4 = -B_4(\hat{t}),$$

(no dependence on N , see eq. (15c)). At a given moment of time we rescale spatial coordinates to set $a = 1$ as we do in Sec. 2.5 and later in the main text. We work in cosmic time with $N = 1$.

We consider various cubic terms in turn.

C1. Triple- ζ action

In the purely scalar sector, the maximum number of spatial derivatives in the cubic action is 4, and the relevant terms, as given in Ref. [45], are

$$\mathcal{S}_{\zeta\zeta\zeta}^{(3)} = \int dt d^3x \left[\Lambda_7 \dot{\zeta} (\partial^2 \zeta)^2 + \Lambda_8 \zeta (\partial^2 \zeta)^2 + \Lambda_9 \partial^2 \zeta (\partial_i \zeta)^2 + \Lambda_{10} \dot{\zeta} (\partial_i \partial_j \zeta)^2 + \Lambda_{11} \zeta (\partial_i \partial_j \zeta)^2 \right],$$

where, as before, $\partial^2 = \partial_i \partial_i$ is the spatial Laplacian, and

$$\Lambda_8 = -\Lambda_{11} = -\frac{3\mathcal{G}_T^3}{2\Theta^2}, \quad (75a)$$

$$\Lambda_9 = -\frac{2\mathcal{G}_T^3}{\Theta^2}, \quad (75b)$$

with $\Lambda_7 = -\Lambda_{10}$. The function Θ , entering (75), is given by (74b), and for the solution in Sec. 2.2, the expression for Θ reduces to (43).

One notices that terms with Λ_7 and Λ_{10} cancel out upon integration by parts (using $\Lambda_7 = -\Lambda_{10}$ and neglecting the term of order $\dot{\Lambda}_{10} \partial_i \partial_j \zeta \partial_i \zeta \partial_j \zeta$). Moreover, among the remaining three monomials, only two are independent, modulo integration by parts, since

$$\int d^3x \zeta (\partial_i \partial_j \zeta)^2 = \int d^3x \left[\zeta (\partial^2 \zeta)^2 + \frac{3}{2} \partial^2 \zeta (\partial_i \zeta)^2 \right].$$

Making use of (75a), one finds that the relevant part of the triple- ζ action has just one term

$$\mathcal{S}_{\zeta\zeta\zeta}^{(3)} = \int dt d^3x \Lambda_\zeta \partial^2 \zeta (\partial_i \zeta)^2, \quad (76)$$

where

$$\Lambda_\zeta = \Lambda_9 - \frac{3}{2} \Lambda_8 = \frac{\mathcal{G}_T^3}{4\Theta^2}.$$

C2. $h\zeta\zeta$, $hh\zeta$ and triple- h actions

In general Horndeski theory with $G_5 \neq 0$, and/or $G_4 = G_4(\phi, X)$, the cubic $h\zeta\zeta$ action has the following general form (see Ref. [68] where explicit expressions are given)

$$\mathcal{S}_{\zeta\zeta h}^{(3)} = \int dt d^3x \left[c_1 h_{ij} \zeta_{,i} \zeta_{,j} + c_2 \dot{h}_{ij} \zeta_{,i} \zeta_{,j} + c_3 \dot{h}_{ij} \zeta_{,i} \psi_{,j} + c_4 \partial^2 h_{ij} \zeta_{,i} \psi_{,j} + c_5 \partial^2 h_{ij} \zeta_{,i} \zeta_{,j} + c_6 \partial^2 h_{ij} \psi_{,i} \psi_{,j} \right],$$

where

$$\psi = \partial^{-2} \partial_t \zeta .$$

The term with c_5 involves 4 spatial derivatives. However, in the particular case that we consider, $G_5 = 0$, $G_4 = G_4(\phi)$, we have

$$c_4 = c_5 = 0 .$$

So, the cubic $h\zeta\zeta$ action involves 2 spatial derivatives only.

The general structure of the cubic ζhh action is [68]

$$\begin{aligned} \mathcal{S}_{\zeta hh}^{(3)} = \int dt d^3x & \left[d_1 \zeta \dot{h}_{ij}^2 + \frac{d_2}{a^2} \zeta h_{ij,k} h_{ij,k} + d_3 \psi_{,k} \dot{h}_{ij} h_{ij,k} + d_4 \dot{\zeta} \dot{h}_{ij}^2 \right. \\ & \left. + \frac{d_5}{a^2} \partial^2 \zeta \dot{h}_{ij}^2 + d_6 \psi_{,ij} \dot{h}_{ik} \dot{h}_{jk} + \frac{d_7}{a^2} \zeta_{,ij} \dot{h}_{ik} \dot{h}_{jk} \right] , \end{aligned}$$

and in our case we have

$$d_4 = d_5 = d_6 = d_7 = 0 .$$

The cubic ζhh action also involves at most 2 spatial derivatives.

The cubic action with tensor modes only is given by (39). It involves at most 2 spatial derivatives as well.

Appendix D. Covariant Lagrangian functions

In this Appendix we collect concrete expressions of covariant coupling functions G_2 , G_3 and G_4 for the contraction stage model (15) with (61). We have already started this procedure in Sec. 2.4, so we start with obtained formulas (37). Substituting concrete expressions for a_2 and a_3 in eq. (37) we arrive to

$$A_2 = \hat{g} e^{(2\mu+2)\phi} a_2 \left(\frac{e^\phi}{\sqrt{2X}} \right) = \hat{g} e^{(2\mu+2)\phi} (c_2 + \sqrt{2X} d_2 e^{-\phi}) , \quad (77a)$$

$$A_3 = \hat{g} e^{(2\mu+1)\phi} a_3 \left(\frac{e^\phi}{\sqrt{2X}} \right) = \hat{g} e^{(2\mu+1)\phi} (c_3 + \sqrt{2X} d_3 e^{-\phi}) , \quad (77b)$$

$$A_4 = -\frac{\hat{g}}{2} e^{2\mu\phi} . \quad (77c)$$

The relationship between the Lagrangian functions in the covariant and ADM formalisms is given by formulas (9) and (11). For completeness, we write an expression for F_X :

$$F_X = -\frac{\hat{g} e^{2\mu\phi} \left(\sqrt{2} c_3 e^\phi + 2(d_3 + 2\mu) \sqrt{X} \right)}{4X^{3/2}} .$$

Substituting the latter formula together with (77) into formulas (9), we immediately arrive to the following covariant Lagrangian functions

$$G_2 = \hat{g}e^{2\mu\phi} \left[e^\phi (c_2 e^\phi + \sqrt{2}(d_2 - c_3 - 2c_3\mu)\sqrt{X}) + 2\mu(d_3 + 2\mu)X \ln X \right], \quad (78a)$$

$$G_3 = \frac{1}{2} \hat{g}e^{2\mu\phi} (d_3 + 2\mu)(2 + \ln X), \quad (78b)$$

$$G_4 = \frac{1}{2} \hat{g}e^{2\mu\phi}. \quad (78c)$$

Next, we find the covariant coupling functions in Einstein frame as well. To this end we will use formulas from Ref. [78], Appendix A.5. Using similar notations as in Ref. [78], we rewrite conformal transformation of the metric as

$$g_{\mu\nu}^{(E)} = e^{2K(\phi)} g_{\mu\nu}, \quad (79)$$

We stick to the action (7) but with $G_4 \equiv G_4(\phi)$ in Jordan frame, while in Einstein frame we demand

$$\mathcal{S} = \int d^4x \sqrt{-g^{(E)}} \left\{ G_2^{(E)}(\phi, X_{(E)}) - G_3^{(E)}(\phi, X_{(E)}) (\square\phi)^{(E)} + \frac{M_P^2}{2} R_{(E)} \right\}, \quad (80)$$

where (E) is just a sub- or superscript meaning Einstein frame. One immediately writes

$$X_{(E)} = -\frac{1}{2} g_{(E)}^{\mu\nu} \partial_\mu \phi \partial_\nu \phi = e^{-2K} X, \quad (81)$$

and

$$\sqrt{-g^{(E)}} = e^{4K} \sqrt{-g}. \quad (82)$$

Next, one can find

$$(\square\phi)^{(E)} = g_{(E)}^{\mu\nu} \nabla_\mu^{(E)} \partial_\nu \phi = e^{-2K} [\square\phi + 2g^{\mu\nu} \partial_\mu K \partial_\nu \phi], \quad (83)$$

where we use formula for the relationship between the Christoffel symbols from Ref. [78]. The relation between scalar curvatures in Einstein and Jordan frame is also given in Ref. [78]. Finally, as a result of substituting these expressions (81)-(83) in eq. (80) and straightforward (but tedious) calculation we obtain

$$\begin{aligned} G_2^{(E)} &= \frac{M_P^4 G_2(\phi, X)}{(2G_4)^2} - \frac{4M_P^4}{(2G_4)^3} G_3(\phi, X) G_{4\phi} X + 12M_P^2 \frac{G_{4\phi}^2}{(2G_4)^3} X, \\ G_3^{(E)} &= M_P^2 \frac{G_3(\phi, X)}{2G_4(\phi)}, \\ G_4^{(E)} &= \frac{M_{Pl}^2}{2}. \end{aligned}$$

It is worth stressing, that during the calculation of formulas for $G_2^{(E)}$, $G_3^{(E)}$, and $G_4^{(E)}$ we obtain that function $K(\phi)$ from (79) is

$$K(\phi) = \frac{1}{2} \ln \left(\frac{2G_4}{M_P^2} \right),$$

which for sure coincides with eq. (25). Finally, if $\frac{M_P^2}{2} = 1$, we arrive to

$$G_2^{(E)} = \frac{G_2}{G_4^2} - 2 \frac{G_{4\phi}}{G_4^3} G_3 X + 3 \frac{G_{4\phi}^2}{G_4^3} X, \quad (84a)$$

$$G_3^{(E)} = \frac{G_3}{G_4}, \quad (84b)$$

$$G_4^{(E)} = 1. \quad (84c)$$

Substituting Jordan frame coupling functions (78) into (84), we find the desired Lagrangian functions in Einstein frame

$$G_2^{(E)} = \frac{4e^{-2\mu\phi}}{\hat{g}} (c_2 e^{2\phi} + \sqrt{2X} d_2 e^\phi - \sqrt{2X} c_3 (2\mu + 1) e^\phi - 4d_3 \mu X - 2\mu^2 X),$$

$$G_3^{(E)} = (d_3 + 2\mu)(2 + \ln X).$$

Appendix E. Scale factor and Hubble parameter in Einstein frame

In this Appendix we show precise calculations of scale factor and Hubble parameter in the case of the model with $\mu = 1$ from Sec. 3.2 in Einstein frame.

We remind that we proceed with the conformal transformation of the metric given by (25). That is why, for scale factor in Einstein frame we have

$$a_E = a \sqrt{\frac{2B_4}{M_{Pl}^2}} = (-t)^{\chi-1} \frac{d\sqrt{g}}{M_{Pl}} \equiv (-t)^{\chi-1} dg_1 = \frac{g_1}{(1-\chi)(-\eta)},$$

where we remind that a is a scale factor in Jordan frame. For the last equality we use more accurate (than we have already written in Sec. 1) formula for the relation between cosmic time in Jordan frame and conformal time:

$$(-t) = [d(1-\chi)(-\eta)]^{\frac{1}{1-\chi}}.$$

We also introduce $g_1 \equiv \frac{\sqrt{g}}{M_{Pl}}$ for simplicity. Note, that the dimension of the latter is -1 . Next, we find cosmic time in Einstein frame

$$t_E = \int_{-\infty}^0 a_E d\eta = -\frac{g_1}{(1-\chi)} \ln(-d^{1/\chi} \eta),$$

and, vice versa

$$(-\eta) = \frac{1}{d^{1/\chi}} e^{-(1-\chi)\frac{t_E}{g_1}}.$$

Finally, the scale factor in Einstein frame in terms of cosmic time t_E is

$$a_E = \frac{g_1}{(1-\chi)} d^{1/\chi} e^{(1-\chi)\frac{t_E}{g_1}}.$$

This scale factor $\frac{a_E(1-\chi)}{g_1 d^{1/\chi}}$ as a function of $\frac{t_E(1-\chi)}{g_1}$ is shown in Fig. 11. The Hubble parameter in Einstein frame is given by

$$H_E \equiv \frac{da_E}{a_E dt_E} = \frac{1-\chi}{g_1}.$$

As it was discussed in Sec. 1, we indeed obtain exponential expansion in Einstein frame in this case.

Appendix F. Stable and subluminal cosmology: contraction, bounce and subsequent GR kination

In this Appendix we give a numerical example of stable and subluminal evolution from contraction stage to bounce and then to kination. The main idea is to “sew” already constructed healthy bounce model from Sec. 3.1 with the subsequent kination epoch from [47] (see Sec. 3.3 within), with the contraction stage from this work given by the Lagrangian (15), (61a), (61b). In this model, the Einstein-Hilbert action for gravity is restored during the kination epoch. To this end, following Ref. [47], we end up with the following example of Lagrangian functions:

$$A_2(\hat{t}, N) = U_2(\hat{t}) \cdot \hat{g} \cdot f(\hat{t})^{-2\mu-2} a_2(N) + \frac{1}{2} (1 - U_2(\hat{t})) f_1(\hat{t})^{-2\mu_1-2} \left(\frac{x(\hat{t})}{N(\hat{t})^2} + \frac{v(\hat{t})}{N(\hat{t})^4} \right), \quad (85a)$$

$$A_3(\hat{t}, N) = U_3(\hat{t}) \cdot \hat{g} \cdot f(\hat{t})^{-2\mu-1} a_3(N) + \frac{1}{2} (1 - U_3(\hat{t})) f_1(\hat{t})^{-2\mu_1-1} \frac{y(\hat{t})}{N(\hat{t})^3} + \frac{V_3(\hat{t})}{N(\hat{t})^2}, \quad (85b)$$

$$A_4(\hat{t}) = -B_4(\hat{t}) = -\frac{1}{2} U_4(\hat{t}) \cdot \hat{g} \cdot f(\hat{t})^{-2\mu} - \frac{1}{2} (1 - U_4(\hat{t})) f_1(\hat{t})^{-2\mu_1} + V_4(\hat{t}). \quad (85c)$$

We construct these functions, following the same logic as in Ref. [47], so that to obtain a smooth transition from contraction to bounce and then to GR kination stage. We set from the beginning

$$\hat{g} = 1.$$

Next, one should choose such n_S and χ from the space of parameters in Fig. 6, which satisfy necessary conditions (68) and (70) from Sec. 3.1. We thus set

$$n_S = 0.967, \quad \chi = 0.4,$$

and using (31) we also find

$$\mu = 1.0099 .$$

We use the same value of μ_1 as in [47]

$$\mu_1 = 0.8 .$$

The functions U_2 , U_3 and U_4 in eqs. (85) are given by

$$U_2(\hat{t}) = 1 + \ln \left(\frac{e^{3.4s(-\hat{t}-55)} + e}{e^{3.4s(-\hat{t}-55)} + e^2} \right), \quad (86a)$$

$$U_3(\hat{t}) = 1 + \ln \left(\frac{e^{5s(-\hat{t}-28)} + e}{e^{5s(-\hat{t}-28)} + e^2} \right), \quad (86b)$$

$$U_4(\hat{t}) = 1 + \ln \left(\frac{e^{4s(-\hat{t}-50)} + e}{e^{4s(-\hat{t}-50)} + e^2} \right), \quad (86c)$$

which were again constructed in the same manner as in Ref. [47] and chosen so that to obtain stable and subluminal evolution at all times: contraction at large negative times, then bounce and kination at large positive times. In eqs. (86) we set $s = 1/500$. Function $f(\hat{t})$ in eqs. (85) is given by

$$f(\hat{t}) = \frac{1}{2} \left((-\hat{t} + 500) + \frac{\ln(2\cosh(s(\hat{t} - 500)))}{s} \right) + c ,$$

with $c = 7$. Next, function f_1 is [47]

$$f_1(\hat{t}) = \frac{c_1}{2} \left(-\hat{t} + \frac{\ln(2\cosh(s\hat{t}))}{s} \right) + 1 ,$$

and $c_1 = 4 \cdot 10^{-3}$. Functions $x(\hat{t})$, $v(\hat{t})$ and $y(\hat{t})$ are the same as in [47]

$$\begin{aligned} x(t) &= x_0(1 - U_x(t)) + \frac{4}{3((t + 2000)^2 + (t - 5000)^2)} \cdot U_x(t), \\ v(t) &= v_0(1 - U_x(t)) + \frac{v_2}{(|t| + 2000)^5} \cdot U_x(t), \\ y(t) &= y_0(1 - U_y(t)) + \frac{y_2}{(|t| + 2000)^5} \cdot U_y(t), \end{aligned}$$

where

$$\begin{aligned} U_x(t) &= \ln \left(\frac{e^{-1.5 \cdot s \cdot (t-80)} + e^2}{e^{-1.5 \cdot s \cdot (t-80)} + e} \right), \\ U_y(t) &= \ln \left(\frac{e^{-3.8 \cdot s \cdot (t+180)} + e^2}{e^{-3.8 \cdot s \cdot (t+180)} + e} \right), \end{aligned}$$

with the following parameters

$$\begin{aligned} x_0 &= -1.6 \cdot 10^{-5}, & y_0 &= -1.2 \cdot 10^{-3}, \\ v_0 &= 5.19 \cdot 10^{-6}, \\ v_2 &= 1.04 \cdot 10^8, & y_2 &= 9.6 \cdot 10^{10}. \end{aligned}$$

Finally, we use two auxiliary functions V_3 and V_4 in eqs. (85)

$$\begin{aligned} V_3(\hat{t}) &= -1.5 \left[1 + \ln \left(\frac{e^{5.15s(-\hat{t}-2100)} + e}{e^{5.15s(-\hat{t}-2100)} + e^2} \right) \right] \left[1 + \ln \left(\frac{e^{5.2s(\hat{t}-70)} + e}{e^{5.2s(\hat{t}-70)} + e^2} \right) \right], \\ V_4(\hat{t}) &= -1.5 \cdot 10^4 \left[1 + \ln \left(\frac{e^{5.15s(-\hat{t}-2300)} + e}{e^{5.15s(-\hat{t}-2300)} + e^2} \right) \right] \left[1 + \ln \left(\frac{e^{5.2s(\hat{t}-70)} + e}{e^{5.2s(\hat{t}-70)} + e^2} \right) \right], \end{aligned}$$

which are needed to proceed stable behaviour near bounce.

Solving equations (71) with chosen functions (85) and with setting

$$\kappa = 1, \quad c_3 = -5, \quad d_3 = -2,$$

which is chosen so that to satisfy necessary conditions (68) and (70) from Sec. 3.1. One can also obtain, using formulas (65), (66), and (67) from Sec. 3.1

$$\rho = 0.053, \quad N_{\text{init}} = \frac{2}{\kappa} (1 + 2\mu - 2(\mu - 1)\chi) = 6.024.$$

Having set Lagrangian functions and all parameters we find Hubble parameter $H(\hat{t})$ and lapse function $N(\hat{t})$ as a solution. Note, that the initial conditions are

$$N(\hat{t}_1) = N_{\text{init}}, \quad H(\hat{t}_1) = \frac{\chi}{N_{\text{init}} \hat{t}_1},$$

where \hat{t}_1 is some numerically suitable large negative time. We show the behavior of Hubble parameter and lapse function at contraction, bounce, and kination in Fig. 12. The scalar coefficients \mathcal{F}_S and \mathcal{G}_S (73) are shown in Fig. 13 and scalar sound speed squared $u_S^2 \equiv \frac{\mathcal{F}_S}{\mathcal{G}_S}$ (24) is shown in Fig. 14 (right one); the stability and subluminality are explicit. We show tensor coefficient \mathcal{F}_T (72) for completeness in Fig. 14 (left one). We recall that $\mathcal{F}_T = \mathcal{G}_T$ (72) and $c_T = 1$ at all times.

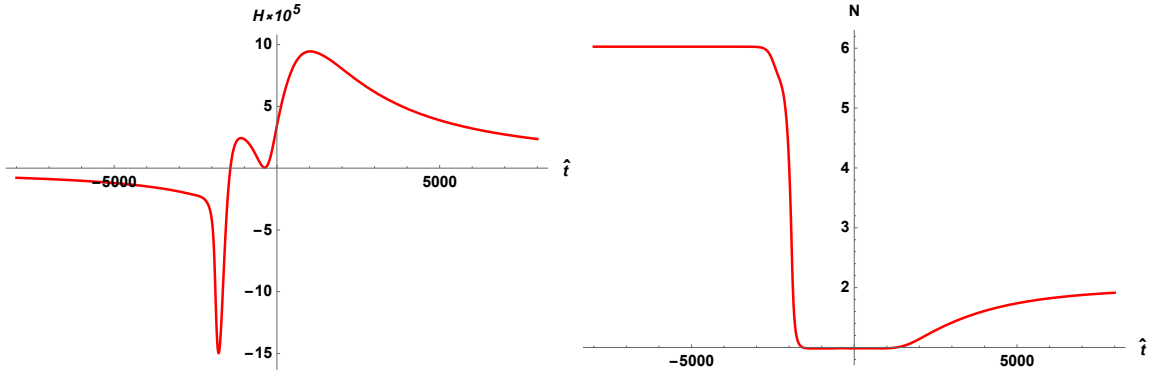


Figure 12: Hubble parameter (left panel) and lapse function (right panel) for the model of Appendix F: contraction, bounce and subsequent GR kination.

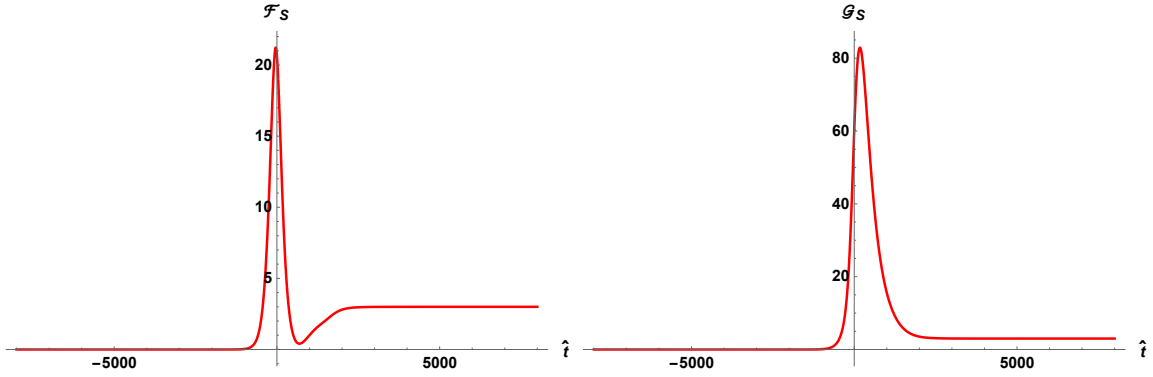


Figure 13: Coefficients \mathcal{F}_S (left panel) and \mathcal{G}_S (right panel) for the model of Appendix F: contraction, bounce and subsequent GR kination.

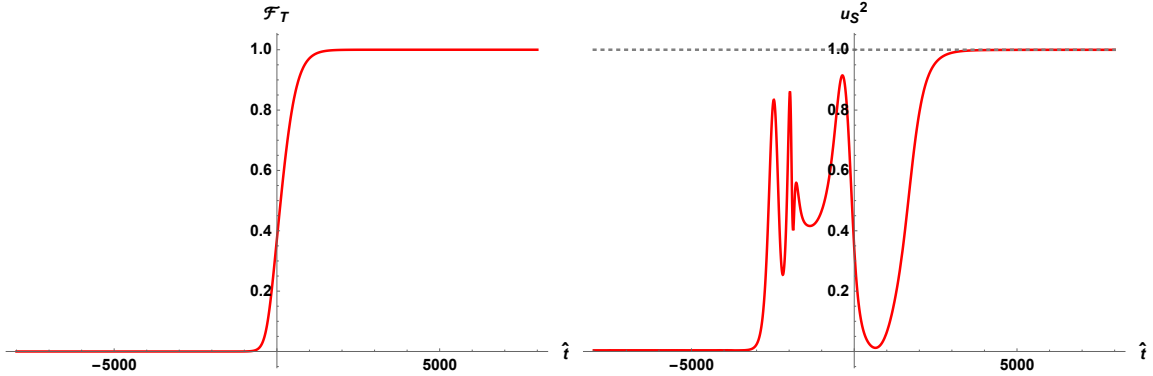


Figure 14: Coefficient \mathcal{F}_T (left panel) and u_S^2 (right panel) for the model of Appendix F: contraction, bounce and subsequent GR kination.

Let us note, that at $\hat{t} \rightarrow +\infty$ we have the following asymptotic behaviour of A_4 in

eq. (85c)

$$A_4 \rightarrow -\frac{1}{2},$$

i.e. we set $M_P = 1$, which means that general relativity is restored at future times in our model.

Finally, one can make sure that the wavelength of primordial fluctuations stretches enough at the end of the contracting phase and before the universe bounces. To this end, we show when our modes exit effective horizon at contracting stage and calculate the number e-folds of contraction.

Consider modes whose *present* wave vector is p_0 , roughly $p_0 \sim H_0$. Suppose, that bounce occurs at scale factor $a = a_b$, and before that the scale factor decreased as (17). Thus,

$$a_b = d|t_b|^\chi,$$

where t_b is the end of contraction stage. The exit of a mode with conformal momentum $k = p_0 a_0$ occurs at (see eq. (28))

$$|t_f| \sim \left(\frac{d}{k}\right)^{\frac{1}{1-\chi}},$$

where we omit the dependence on sound speed u_s . Next, one can write

$$k = p_0 a_0 = p_0 \frac{a_0}{a_b} d|t_b|^\chi,$$

and obtain

$$|t_f| \sim \left(\frac{1}{p_0 \frac{a_0}{a_b} |t_b|^\chi}\right)^{\frac{1}{1-\chi}}.$$

We now make use of the fact that at contracting epoch we have $H(t) \sim 1/|t|$ (which is valid also at t_b) and get

$$|t_f| \sim |t_b| \cdot \left(\frac{H_b a_b}{p_0 a_0}\right)^{\frac{1}{1-\chi}},$$

which, for $p_0 \sim H_0$, gives finally

$$|t_f| \sim |t_b| \cdot \left(\frac{H_b a_b}{H_0 a_0}\right)^{\frac{1}{1-\chi}}.$$

If $(H_0 a_0)/(H_b a_b) \ll 1$ is satisfied for the model, then horizon exit occurs long before the bounce. Thus, further we estimate the value of $(H_0 a_0)/(H_b a_b)$ in the model with the Lagrangian functions (85). Firstly, we can immediately write the values of Hubble parameters

$$\begin{aligned} H_0 &\sim 10^2 \cdot \text{km} \cdot \text{s}^{-1} \cdot \text{Mpc}^{-1} \sim 10^{-61}, \\ H_b &\sim 4.2 \cdot 10^{-5}, \end{aligned}$$

where we remind that we work in terms of $M_P = 1$. Here, for H_0 we take some rough estimated value, and H_b is obtained numerically at $\hat{t}_b \approx -2000$.⁶ Note, that we define this moment of time \hat{t}_b as a moment from which the formula for Hubble parameter $H \sim 1/|\hat{t}|$ becomes irrelevant. Next, we find a_0 . It can be roughly estimated as

$$a_0 \approx a_e \frac{T_{reh}}{T_0},$$

where a_e is the scale factor in the end of the bounce and we suppose that reheating occurs instantly after the bounce. This a_e is given by

$$a_e \approx a_b \left(\int_{\hat{t}_b}^{\hat{t}_{\text{cross}}} NH d\hat{t} + \int_{\hat{t}_{\text{cross}}}^{\hat{t}_e} NH d\hat{t} \right) \equiv a_b (I_1 + I_2),$$

where we remind that $\hat{t}_b = -2000$ and we also set $\hat{t}_e = 2000$ (approximate time when the bounce ends), while $\hat{t}_{\text{cross}} \approx -1450$ is a moment of time, where Hubble parameter changes the sign. The integrals are calculated numerically and equal

$$I_1 \approx -0.07, \quad I_2 \approx 0.2.$$

Finally, we write

$$\frac{H_b a_b}{H_0 a_0} \approx \frac{H_b \cdot T_0}{H_0 \cdot I \cdot T_{reh}}.$$

Choosing, say, $T_{reh} = 10^{-12} M_P$, and having $T_0 \approx 10^{-32} M_P$ we arrive to

$$\frac{H_b a_b}{H_0 a_0} \approx 10^{37} \gg 1,$$

so, we have proved that the horizon exit occurs long before the bounce.

Let us estimate the number of e-folds \mathcal{N} which can be gained during contraction epoch. This is given by

$$e^{\mathcal{N}} \equiv \frac{a(t_f)}{a_b} = \frac{|t_f|^\chi}{|t_b|^\chi} = \left(\frac{H_b a_b}{H_0 a_0} \right)^{\frac{\chi}{1-\chi}},$$

so

$$\mathcal{N} = \frac{\chi}{1-\chi} \ln \left(\frac{H_b a_b}{H_0 a_0} \right) \approx 58,$$

so our model is physically relevant, i.e. the wavelength of primordial fluctuations stretches ~ 60 Hubble scales at the end of the contracting phase and before the universe bounces.

⁶We recall that $\hat{t} = \int \frac{dt}{N(\hat{t})}$.

References

- [1] V. A. Rubakov, Phys. Usp. **57** (2014), 128-142 doi:10.3367/UFNe.0184.201402b.0137 [arXiv:1401.4024 [hep-th]].
- [2] F. J. Tipler, Phys. Rev. D **17** (1978), 2521-2528 doi:10.1103/PhysRevD.17.2521
- [3] P. Creminelli, A. Nicolis and E. Trincherini, JCAP **11** (2010), 021 doi:10.1088/1475-7516/2010/11/021 [arXiv:1007.0027 [hep-th]].
- [4] C. Deffayet, O. Pujolas, I. Sawicki and A. Vikman, JCAP **10** (2010), 026 doi:10.1088/1475-7516/2010/10/026 [arXiv:1008.0048 [hep-th]].
- [5] T. Kobayashi, M. Yamaguchi and J. Yokoyama, Phys. Rev. Lett. **105** (2010), 231302 doi:10.1103/PhysRevLett.105.231302 [arXiv:1008.0603 [hep-th]].
- [6] G. W. Horndeski, Int. J. Theor. Phys. **10** (1974), 363-384 doi:10.1007/BF01807638
- [7] T. Kobayashi, Rept. Prog. Phys. **82** (2019) no.8, 086901 doi:10.1088/1361-6633/ab2429 [arXiv:1901.07183 [gr-qc]].
- [8] M. Novello and S. E. P. Bergliaffa, Phys. Rept. **463** (2008), 127-213 doi:10.1016/j.physrep.2008.04.006 [arXiv:0802.1634 [astro-ph]].
- [9] J. L. Lehners, Phys. Rept. **465** (2008), 223-263 doi:10.1016/j.physrep.2008.06.001 [arXiv:0806.1245 [astro-ph]].
- [10] J. L. Lehners, Class. Quant. Grav. **28** (2011), 204004 doi:10.1088/0264-9381/28/20/204004 [arXiv:1106.0172 [hep-th]].
- [11] D. Battfeld and P. Peter, Phys. Rept. **571** (2015), 1-66 doi:10.1016/j.physrep.2014.12.004 [arXiv:1406.2790 [astro-ph.CO]].
- [12] T. Qiu, J. Evslin, Y. F. Cai, M. Li and X. Zhang, JCAP **10** (2011), 036 doi:10.1088/1475-7516/2011/10/036 [arXiv:1108.0593 [hep-th]].
- [13] D. A. Easson, I. Sawicki and A. Vikman, JCAP **11** (2011), 021 doi:10.1088/1475-7516/2011/11/021 [arXiv:1109.1047 [hep-th]].
- [14] Y. F. Cai, D. A. Easson and R. Brandenberger, JCAP **08** (2012), 020 doi:10.1088/1475-7516/2012/08/020 [arXiv:1206.2382 [hep-th]].
- [15] M. Osipov and V. Rubakov, JCAP **11** (2013), 031 doi:10.1088/1475-7516/2013/11/031 [arXiv:1303.1221 [hep-th]].

- [16] T. Qiu, X. Gao and E. N. Saridakis, *Phys. Rev. D* **88** (2013) no.4, 043525 doi:10.1103/PhysRevD.88.043525 [arXiv:1303.2372 [astro-ph.CO]].
- [17] M. Koehn, J. L. Lehners and B. A. Ovrut, *Phys. Rev. D* **90** (2014) no.2, 025005 doi:10.1103/PhysRevD.90.025005 [arXiv:1310.7577 [hep-th]].
- [18] L. Battarra, M. Koehn, J. L. Lehners and B. A. Ovrut, *JCAP* **07** (2014), 007 doi:10.1088/1475-7516/2014/07/007 [arXiv:1404.5067 [hep-th]].
- [19] T. Qiu and Y. T. Wang, *JHEP* **04** (2015), 130 doi:10.1007/JHEP04(2015)130 [arXiv:1501.03568 [astro-ph.CO]].
- [20] A. Ijjas and P. J. Steinhardt, *Phys. Rev. Lett.* **117** (2016) no.12, 121304 doi:10.1103/PhysRevLett.117.121304 [arXiv:1606.08880 [gr-qc]].
- [21] R. Brandenberger and P. Peter, *Found. Phys.* **47** (2017) no.6, 797-850 doi:10.1007/s10701-016-0057-0 [arXiv:1603.05834 [hep-th]].
- [22] A. Ijjas and P. J. Steinhardt, *Class. Quant. Grav.* **35** (2018) no.13, 135004 doi:10.1088/1361-6382/aac482 [arXiv:1803.01961 [astro-ph.CO]].
- [23] S. Mironov, V. Rubakov and V. Volkova, doi:10.1134/S00444451019100079 [arXiv:1906.12139 [hep-th]].
- [24] P. Creminelli, K. Hinterbichler, J. Khoury, A. Nicolis and E. Trincherini, *JHEP* **02** (2013), 006 doi:10.1007/JHEP02(2013)006 [arXiv:1209.3768 [hep-th]].
- [25] K. Hinterbichler, A. Joyce, J. Khoury and G. E. J. Miller, *JCAP* **12** (2012), 030 doi:10.1088/1475-7516/2012/12/030 [arXiv:1209.5742 [hep-th]].
- [26] B. Elder, A. Joyce and J. Khoury, *Phys. Rev. D* **89** (2014) no.4, 044027 doi:10.1103/PhysRevD.89.044027 [arXiv:1311.5889 [hep-th]].
- [27] D. Pirtskhalava, L. Santoni, E. Trincherini and P. Uttayarat, *JHEP* **12** (2014), 151 doi:10.1007/JHEP12(2014)151 [arXiv:1410.0882 [hep-th]].
- [28] S. Nishi and T. Kobayashi, *JCAP* **03** (2015), 057 doi:10.1088/1475-7516/2015/03/057 [arXiv:1501.02553 [hep-th]].
- [29] T. Kobayashi, M. Yamaguchi and J. Yokoyama, *JCAP* **07** (2015), 017 doi:10.1088/1475-7516/2015/07/017 [arXiv:1504.05710 [hep-th]].
- [30] M. Libanov, S. Mironov and V. Rubakov, *JCAP* **08** (2016), 037 doi:10.1088/1475-7516/2016/08/037 [arXiv:1605.05992 [hep-th]].

- [31] T. Kobayashi, Phys. Rev. D **94** (2016) no.4, 043511 doi:10.1103/PhysRevD.94.043511 [arXiv:1606.05831 [hep-th]].
- [32] R. Kolevator and S. Mironov, Phys. Rev. D **94** (2016) no.12, 123516 doi:10.1103/PhysRevD.94.123516 [arXiv:1607.04099 [hep-th]].
- [33] S. Akama and T. Kobayashi, Phys. Rev. D **95** (2017) no.6, 064011 doi:10.1103/PhysRevD.95.064011 [arXiv:1701.02926 [hep-th]].
- [34] Y. Cai and Y. S. Piao, JHEP **09** (2017), 027 doi:10.1007/JHEP09(2017)027 [arXiv:1705.03401 [gr-qc]].
- [35] R. Kolevator, S. Mironov, N. Sukhov and V. Volkova, JCAP **08** (2017), 038 doi:10.1088/1475-7516/2017/08/038 [arXiv:1705.06626 [hep-th]].
- [36] G. Ye and Y. S. Piao, Phys. Rev. D **99** (2019) no.8, 084019 doi:10.1103/PhysRevD.99.084019 [arXiv:1901.08283 [gr-qc]].
- [37] S. Mironov, V. Rubakov and V. Volkova, Phys. Rev. D **100** (2019) no.8, 083521 doi:10.1103/PhysRevD.100.083521 [arXiv:1905.06249 [hep-th]].
- [38] A. Ilyas, M. Zhu, Y. Zheng, Y. F. Cai and E. N. Saridakis, JCAP **09** (2020), 002 doi:10.1088/1475-7516/2020/09/002 [arXiv:2002.08269 [gr-qc]].
- [39] M. Zhu, A. Ilyas, Y. Zheng, Y. F. Cai and E. N. Saridakis, JCAP **11** (2021) no.11, 045 doi:10.1088/1475-7516/2021/11/045 [arXiv:2108.01339 [gr-qc]].
- [40] M. Zumalacárregui and J. García-Bellido, Phys. Rev. D **89** (2014), 064046 doi:10.1103/PhysRevD.89.064046 [arXiv:1308.4685 [gr-qc]].
- [41] J. Gleyzes, D. Langlois, F. Piazza and F. Vernizzi, Phys. Rev. Lett. **114** (2015) no.21, 211101 doi:10.1103/PhysRevLett.114.211101 [arXiv:1404.6495 [hep-th]].
- [42] D. Langlois and K. Noui, JCAP **02** (2016), 034 doi:10.1088/1475-7516/2016/02/034 [arXiv:1510.06930 [gr-qc]].
- [43] S. Mironov, V. Rubakov and V. Volkova, JHEP **04** (2021), 035 doi:10.1007/JHEP04(2021)035 [arXiv:2011.14912 [hep-th]].
- [44] Y. A. Ageeva, O. A. Evseev, O. I. Melichev and V. A. Rubakov, EPJ Web Conf. **191** (2018), 07010 doi:10.1051/epjconf/201819107010 [arXiv:1810.00465 [hep-th]].
- [45] Y. Ageeva, O. Evseev, O. Melichev and V. Rubakov, Phys. Rev. D **102** (2020) no.2, 023519 doi:10.1103/PhysRevD.102.023519 [arXiv:2003.01202 [hep-th]].

- [46] Y. Ageeva, P. Petrov and V. Rubakov, JHEP **12** (2020), 107 doi:10.1007/JHEP12(2020)107 [arXiv:2009.05071 [hep-th]].
- [47] Y. Ageeva, P. Petrov and V. Rubakov, Phys. Rev. D **104** (2021) no.6, 063530 doi:10.1103/PhysRevD.104.063530 [arXiv:2104.13412 [hep-th]].
- [48] D. Nandi, Phys. Lett. B **809** (2020), 135695 doi:10.1016/j.physletb.2020.135695 [arXiv:2003.02066 [astro-ph.CO]].
- [49] D. Nandi, Universe **7** (2021) no.3, 62 doi:10.3390/universe7030062 [arXiv:2009.03134 [gr-qc]].
- [50] N. Aghanim *et al.* [Planck], Astron. Astrophys. **641** (2020), A6 [erratum: Astron. Astrophys. **652** (2021), C4] doi:10.1051/0004-6361/201833910 [arXiv:1807.06209 [astro-ph.CO]].
- [51] G. Ye, B. Hu and Y. S. Piao, Phys. Rev. D **104** (2021) no.6, 063510 doi:10.1103/PhysRevD.104.063510 [arXiv:2103.09729 [astro-ph.CO]].
- [52] J. Q. Jiang and Y. S. Piao, Phys. Rev. D **105** (2022) no.10, 103514 doi:10.1103/PhysRevD.105.103514 [arXiv:2202.13379 [astro-ph.CO]].
- [53] J. Gleyzes, D. Langlois, F. Piazza and F. Vernizzi, JCAP **08** (2013), 025 doi:10.1088/1475-7516/2013/08/025 [arXiv:1304.4840 [hep-th]].
- [54] M. Fasiello and S. Renaux-Petel, JCAP **10** (2014), 037 doi:10.1088/1475-7516/2014/10/037 [arXiv:1407.7280 [astro-ph.CO]].
- [55] E. M. Lifshitz and I. M. Khalatnikov, Adv. Phys. **12** (1963), 185-249 doi:10.1080/00018736300101283
- [56] V. A. Belinsky, I. M. Khalatnikov and E. M. Lifshitz, Adv. Phys. **19** (1970), 525-573 doi:10.1080/00018737000101171
- [57] V. A. Belinskii, E. M. Lifshitz and I. M. Khalatnikov, Zh. Eksp. Teor. Fiz. **62** (1972), 1606-1613
- [58] J. K. Erickson, D. H. Wesley, P. J. Steinhardt and N. Turok, Phys. Rev. D **69** (2004), 063514 doi:10.1103/PhysRevD.69.063514 [arXiv:hep-th/0312009 [hep-th]].
- [59] P. A. R. Ade *et al.* [BICEP and Keck], Phys. Rev. Lett. **127** (2021) no.15, 151301 doi:10.1103/PhysRevLett.127.151301 [arXiv:2110.00483 [astro-ph.CO]].
- [60] M. Tristram, A. J. Banday, K. M. Górski, R. Keskitalo, C. R. Lawrence, K. J. Andersen, R. B. Barreiro, J. Borrill, L. P. L. Colombo and H. K. Eriksen, *et al.* Phys. Rev. D **105** (2022) no.8, 083524 doi:10.1103/PhysRevD.105.083524 [arXiv:2112.07961 [astro-ph.CO]].

- [61] J. Garriga and V. F. Mukhanov, Phys. Lett. B **458** (1999), 219-225 doi:10.1016/S0370-2693(99)00602-4 [arXiv:hep-th/9904176 [hep-th]].
- [62] V. F. Mukhanov and A. Vikman, JCAP **02** (2006), 004 doi:10.1088/1475-7516/2006/02/004 [arXiv:astro-ph/0512066 [astro-ph]].
- [63] D. Langlois, S. Renaux-Petel, D. A. Steer and T. Tanaka, Phys. Rev. Lett. **101** (2008), 061301 doi:10.1103/PhysRevLett.101.061301 [arXiv:0804.3139 [hep-th]].
- [64] X. Gao, T. Kobayashi, M. Yamaguchi and J. Yokoyama, Phys. Rev. Lett. **107** (2011), 211301 doi:10.1103/PhysRevLett.107.211301 [arXiv:1108.3513 [astro-ph.CO]].
- [65] A. De Felice and S. Tsujikawa, JCAP **04** (2011), 029 doi:10.1088/1475-7516/2011/04/029 [arXiv:1103.1172 [astro-ph.CO]].
- [66] X. Gao and D. A. Steer, JCAP **12** (2011), 019 doi:10.1088/1475-7516/2011/12/019 [arXiv:1107.2642 [astro-ph.CO]].
- [67] A. De Felice and S. Tsujikawa, Phys. Rev. D **84** (2011), 083504 doi:10.1103/PhysRevD.84.083504 [arXiv:1107.3917 [gr-qc]].
- [68] X. Gao, T. Kobayashi, M. Shiraishi, M. Yamaguchi, J. Yokoyama and S. Yokoyama, PTEP **2013** (2013), 053E03 doi:10.1093/ptep/ptt031 [arXiv:1207.0588 [astro-ph.CO]].
- [69] J. A. Oller, Prog. Part. Nucl. Phys. **110** (2020), 103728 doi:10.1016/j.pnpnp.2019.103728 [arXiv:1909.00370 [hep-ph]].
- [70] J. A. Oller, *A Brief Introduction to Dispersion Relations. With modern Applications* (Springer Briefs in Physics, Heidelberg, 2019)
- [71] A. Lacour, J. A. Oller and U. G. Meissner, Annals Phys. **326** (2011), 241-306 doi:10.1016/j.aop.2010.06.012 [arXiv:0906.2349 [nucl-th]].
- [72] D. Gülmez, U. G. Meißner and J. A. Oller, Eur. Phys. J. C **77** (2017) no.7, 460 doi:10.1140/epjc/s10052-017-5018-z [arXiv:1611.00168 [hep-ph]].
- [73] Y. A. Ageeva and P. K. Petrov, Phys. Usp. **66** (2023) no.11, 1134-1141 doi:10.3367/UFNe.2022.11.039259 [arXiv:2206.03516 [hep-th]].
- [74] C. Grojean, Phys. Usp. **50** (2007), 1-35 doi:10.1070/PU2007v050n01ABEH006157
- [75] C. Armendariz-Picon, T. Damour and V. F. Mukhanov, Phys. Lett. B **458** (1999), 209-218 doi:10.1016/S0370-2693(99)00603-6 [arXiv:hep-th/9904075 [hep-th]].

- [76] H. Bazrafshan Moghaddam, R. Brandenberger and J. Yokoyama, *Phys. Rev. D* **95** (2017) no.6, 063529 doi:10.1103/PhysRevD.95.063529 [arXiv:1612.00998 [hep-th]].
- [77] T. Kobayashi, M. Yamaguchi and J. Yokoyama, *Prog. Theor. Phys.* **126** (2011), 511-529 doi:10.1143/PTP.126.511 [arXiv:1105.5723 [hep-th]].
- [78] V. A. Rubakov and D. S. Gorbunov, World Scientific, 2017, ISBN 978-981-320-987-9, 978-981-320-988-6, 978-981-322-005-8 doi:10.1142/10447